



VLAKNA TEXTIL

2

Ročník 20.
2013

ISSN1335-0617

Indexed in:

Chemical
Abstracts,

World Textile
Abstracts

EMDASE

Elsevier
Biobase

Elsevier
GeoAbstracts



FIBRES AND TEXTILES VLÁKNA A TEXTIL

Vydáva

- Slovenská technická univerzita v Bratislave, Fakulta chemickej a potravinárskej technológie
- Technická univerzita v Liberci, Fakulta textilní
- Trenčianska univerzita A. Dubčeka v Trenčíne, Fakulta priemyselných technológií
- Výskumný ústav chemických vlákien, a.s. Svit
- Slovenská spoločnosť priemyselnej chémie, Bratislava
- VÚTCH – CHEMITEX, spol. s r.o., Žilina

Published by

- Slovak University of Technology in Bratislava, Faculty of Chemical and Food Technology
- Technical University of Liberec, Faculty of Textile Engineering
- A. Dubček University in Trenčín, Faculty of Industrial Technologies
- Research Institute of Man-Made Fibres, j.s.c., Svit
- Slovak Society of Industrial Chemistry, j.s.c., Bratislava
- VÚTCH – CHEMITEX, Ltd., Žilina

Šéfredaktor (Editor in Chief): A. Ujhelyiová

Redakčná rada

M. Hricová, M. Jambrich, J. Kochan, P. Lizák, P. Michlík, M. Pajtášová, M. Prášil, M. Révus, I. Sroková, V. Váry

Editorial Board

Čestní členovia redakčnej rady

R.U. Bauer (DE), D. Ciechanska (PL), T. Czigani (HU), J. Drašarová (CZ), A.M. Grancarić (HR), M. Krištofič (SK), I. Krucinska (PL), A. Marcinčin (SK), A.M. Marechal (SL), J. Miličský (CZ), R. Redhammer (SK), J. Šajbidor (SK), J. Šesták (SK), M. Budzák (SK), J. Vavro (SK), V. Vlasenko (UA)

Honourable Editorial Board

Výkonný redaktor (Executive Editor): M. Hricová

Redakcia a distribúcia časopisu:
(Editorial Office and distribution of the journal)

STU in Bratislava, FCHPT, Oddelenie vlákien a textilu,
Radlinského 9, 812 37 Bratislava, SK
Tel: 00 421 2 59 325 575
Fax: 00421 2 524 931 98
e-mail: marcela.hricova@stuba.sk

Objednávka a inzercia časopisu:
(Order and advertisement of the journal)

Slovenská spoločnosť priemyselnej chémie,
člen Zväzu vedecko-technických spoločností
Radlinského 9, 812 37 Bratislava, SK
Tel: 00 421 2 59 325 575, Fax: 00421 2 524 931 98
e-mail: marcela.hricova@stuba.sk

Objednávka časopisu zo zahraničia – okrem Českej republiky
Order of the journal from abroad – excepting Czech Republic
SLOVART G.T.G, s.r.o. EXPORT-IMPORT
Krupinská 4, P.O.Box 152, 852 99 Bratislava, SK
Tel: 00421 2 839 471-3, Fax: 00421 2 839 485
e-mail: info@slovart-gtg.sk

Sadzba a tlač

FOART, s.r.o., Bratislava

Typeset and printing at

Časopis vychádza 4x ročne
Ročné predplatné 60 EUR

Journal is published 4x per year
Subscription 60 EUR

Contributions are issued without any proof-readings

ISSN 1335-0617

Evidenčné číslo MKCR SR Bratislava EV 4006/10

Fibres and Textiles (2) 2013

Vlákna a textil (2) 2013

Content	Obsah
FIBRE-FORMING POLYMERS	VLÁKNOTVORNÉ POLYMÉRY
3 <i>A. Marcinčin, K. Marcinčin, M. Hricová, A. Ujhelyiová, J. Janicki and C. Slusarczyk</i> Polypropylene/organoclay composite fibers, structure, thermal and mechanical properties	3 <i>A. Marcinčin, K. Marcinčin, M. Hricová, A. Ujhelyiová, J. Janicki a C. Slusarczyk</i> Polypropylén/organoílové kompozitné vlákna, štruktúra, termické a mechanické vlastnosti
TEXTILE MATERIALS	TEXTILNÉ MATERIÁLY
14 <i>M. Nejedlá</i> Blended textiles with fibers Protex-M for extreme conditions	14 <i>M. Nejedlá</i> Směšové textilie s vlákny Protex-M pro extrémní podmínky
21 <i>E. Moučková, P. Ursíny and P. Jirásková</i> Analysis of cotton blended yarns irregularity	21 <i>E. Moučková, P. Ursíny a P. Jirásková</i> Analýza nestejnóměrnosti směsových bavlnářských přízí
32 <i>B. Kolčavová Sirková</i> Description of binding waves using the Fourier series	32 <i>B. Kolčavová Sirková</i> Popis vazné vlny v provázání s využitím součtu Fourierovy řady
NEWS FROM DEPARTMENTS	Z VEDECKO-VÝSKUMNÝCH A VÝVOJOVÝCH PRACOVÍSK
41 <i>O.V. Kolosnichenko</i> The development approaches to the new forms of clothes creation with signs and symbols of Tripill culture by designing methods	41 <i>O.V. Kolosnichenko</i> Vývoj nových foriem tvorby oblečenia so znakmi Tripillskej kultúry

POLYPROPYLENE/ORGANOCLAY COMPOSITE FIBERS, STRUCTURE, THERMAL AND MECHANICAL PROPERTIES

A. Marcinčin, K. Marcinčin†, M. Hricová, A. Ujhelyiová, J. Janicki* and C. Slusarczyk*

Department of Fibers and Textile Chemistry, Faculty of Chemical and Food Technology, Slovak University of Technology in Bratislava, Radlinskeho 9, 812 37 Bratislava, Slovakia

**Institute of Textile Engineering and Polymer Materials, University of Bielsko-Biala, Willowa 2, 43 309 Bielsko-Biala, Poland
anton.marcincin@stuba.sk*

Abstract: *In this paper, the effect of uniaxial deformation of PP/organoclay composite fibers in spinning and drawing on their supermolecular structure, thermal and mechanical properties is presented. The commercial organoclays Cloisite C15A and Cloisite C30B, both based on montmorillonite (MMT) were used in experimental work as inorganic fillers. The supermolecular structure of fibers was investigated by DSC analysis and X-ray diffraction (WAXS). The DSC measurements were carried out using conventional method (CM) and constant length method (CLM) in which the fibers with constant length during measurement were assured. The average orientation of fibers has been evaluated by the sonic velocity method. Intercalation of polypropylene in the interlayer galleries of organoclay was evaluated by SAXS method. Tenacity and Young's modulus of composite fibers were evaluated and discussed with regard to their thermal properties and supermolecular structure as well as intercalation and exfoliation of (nano)filler in polymer matrix.*

Keywords: *Nanocomposites, Fibers, SAXS, Thermal properties, Mechanical properties*

1 INTRODUCTION

The incorporation of the organoclay into the semicrystalline polymers affects their crystalline properties such as crystallization kinetics, crystal structures and total crystallinity [1, 2]. The layered silicates in the polypropylene (PP) matrix behave as effective heterogeneous nucleating agents. They enhance the crystallization rate [2], and at the same time decrease the spherulite size, perfection of the crystals and shift the cooling crystallization temperature to higher values [3]. Besides, the silicate nanoplatelets affect the shear flow induced crystallization and retardancy of the crystallisation kinetic of matrix at the quiescent crystallization of the PP/montmorillonite (MMT) composites [4-6]. The preferential orientation of PP lamellae perpendicular to the surface of the organoclay layers was found for PP/talc composite by TEM observation [7]. The lamellar orientation on the clay layers was ascribed to nucleation and crystallization at the surface of the silicate platelets. Moreover, the asymmetric morphology of crystals was

observed in PP/organoclay nanocomposites at higher temperature [8] and at shear induced formation of the oriented threadlike crystallites [1]. The high oriented structure elements of fibers are considered in the development of the high tenacity and high modulus of fibers. The advantages of the most semi-crystalline polymers are their ability to self reinforce via the formation of fibrillar structure at deformation at relative high temperature [9-11].

Simultaneously with the development of highly oriented polymers the suitable methods for investigation of the oriented polymer structure were developed or modified [12]. Particularly, the Raman spectroscopy and X-ray diffraction enable investigation of the molecular and crystal deformation of composite fibers in detail [13]. The special method of DSC analysis of fibers, known as "constrain method" or method of "constant length of fibers" (DSC-CLM), has been described in several papers. This DSC method is particularly suitable for evaluation of oriented structure elements of composite fibers [14, 15].

In our previous papers the effect of organoclay on mechanical properties of PP fibers was studied [16, 17]. Surprisingly, the orientation of polymer suppresses the effect of organoclay on tenacity and Young's modulus of composite fibers which is characteristic for isotropic polymer. The positive effect of organoclay on mechanical properties of fibers was found for very low concentration of solid particles only. In this case, the contribution of nanoparticles as hard segments on mechanical properties is negligible. Thus, enhancement of the mechanical properties of composite fibers is affected indirectly by suitable structure obtained at maximal orientation (maximal draw ratio) of fibers. Some convenient methods were used for characterization of structure and morphology of PP composite fibers in our experimental work to explain their mechanical properties. The results are presented in this paper.

2 EXPERIMENTAL

2.1 Material used

Polymers: Two commercially available types of PP were used in the experimental work: polypropylene HPF (*PP HP*) with melt flow index (MFI) 8.0 g/10 min, in powder form and fiber-grade polypropylene TG 920 (*PP*) with MFI 10.5 g/10 min. Both polypropylenes were produced by Slovnaft a. s., Bratislava, Slovak Republic.

Fillers: Two kinds of organoclays (OC) used in this work were Cloisite 15A (*C15A*) and Cloisite 30B (*C30B*), both produced by Southern Clay Product, Inc, Gonzales, TX 78629, USA. C15A is montmorillonite ion exchanged with dimethyl dihydrogenated tallow quarternary ammonium ions. C30B is montmorillonite treated by methyl tallow bis-2-hydroxyl quarternary ammonium ions.

Compatibilisers: Two different non-reactive compatibilisers-dispersants were used for the preparation of concentrated dispersion of organoclay in the PP HP. Commercially available Slovacid 44P (*S44P*) based on the ester of stearic acid and polypropylene glycol, produced by Sasol GmbH, Brunsbüttel,

Germany and Tegopren 6875 (*TEG*) based on poly (alkylsiloxane) produced by Degussa Co., Düsseldorf, Germany.

2.2 Preparation of polypropylene/organoclay composite fiber

1. Preparation of concentrated dispersion of solid particles in PP: The PP HP, organoclay and compatibiliser were mixed in a high rpm mixer for a defined time. Powder mixture was melted and kneaded using twin screw corotating extruder ϕ 28 mm. Temperatures of the extruder zones from feedstock to head were 80, 150, 220, 225, 225, 225 and 232°C. The temperature of the extruded melt was 229°C. The extruded produce was cooled and cut. The concentration of organoclay in PP HP was 10.0 wt.%. Content of compatibiliser was 4.0 wt.%.

2. Melt mixing of concentrated organoclay dispersion with PP using one screw extruder and consequential spinning of PP composite: The chips of organoclay concentrate dispersion and PP were mixed and spun using a single screw extruder ϕ 30 mm and a spinneret with 40 orifices. The spinning temperature was 280°C, metering of melt 30 g/min, spinning speed 360 m/min and the fineness of spun fibers (drawn ratio 1:1, λ_1) was 840 dtex. Fibers were drawn using laboratory drawing machine for draw ratio 1:3 (λ_3) and for maximum drawn ratio (λ_{max}) at drawing temperature 120°C.

2.3 Methods used

DSC measurement: The measurements were performed using Perkin Elmer DSC 7 in the temperature range 30-200°C. The standard heating rate was 10°C/min. The measurements were carried out using conventional method (DSC-CM) in which the cut fibers with length 1-2 mm were used, and constant length method (DSC-CLM) in which the constant length of fibers during measurement was assured. The constant length of the fibers was achieved through winding and fixation of fibers on a wire. The melting peak temperature T_m and melting enthalpy ΔH_m were evaluated.

X-ray scattering method:

Wide-angle scattering (WAXS) method: The structure of fibers was evaluated by a wide-angle X-ray scattering method. The investigations were carried out using a Seifert X-ray diffractometer. On the basis of the WAXS patterns the parameters characterising the fiber structure were determined. The total crystallinity X_{α} and the content of the mesophase X_m were calculated as a ratio of the area under crystalline or mesophase peaks to the total area [18].

Small-angle scattering (SAXS) method: All SAXS patterns were recorded with an MBraun SWAX camera with the Kratky collimation system equipped with a PSD 50 MBraun linear position sensitive detector. The X-ray tube was a conventional copper anode operated at 40 kV and 30 mA controlled by Philips PW 1830 X-ray generator. Cu $K\alpha$ radiation was obtained by filtering with Ni and pulse height discrimination. The powders were measured at room temperature while being kept in a standard sample holder, sealed with aluminium foils.

Orientation of fibers: The average factor of orientation of fibers (f_{α}) was evaluated by sonic velocity measurements using Dynamic Modulus Tester-PPM-5R.

Mechanical properties of the blend fibers: The Instron (3343 model) was used for the measurements of mechanical properties of fibers (according to ISO 2062:1993). They were evaluated from 15 measurements. The initial length of fibers was 25 cm and the time of deformation was about 20 sec.

3 RESULTS AND DISCUSSION

3.1 Thermal properties and supermolecular structure of fibers

The DSC-CM method provides simple one-peak thermogram for undrawn fibers and characteristic double-peak thermogram for middle draw ratio of fibers (Figure 1a).

The radically different shapes of melting endotherms were observed for PP fibers in dependence on the draw ratio using DSC-CLM method. The endotherm peak is shifted to higher temperature gradually when the draw ratio increases (Figure 1b, 1c). One-peak endotherm becomes wider with the increase of draw ratio.

The melting temperature (T_m) and melting enthalpy ΔH_m for PP fibers and for PP/organoclay composite fibers increase proportionally with the draw ratio up to maximum values (Figure 2).

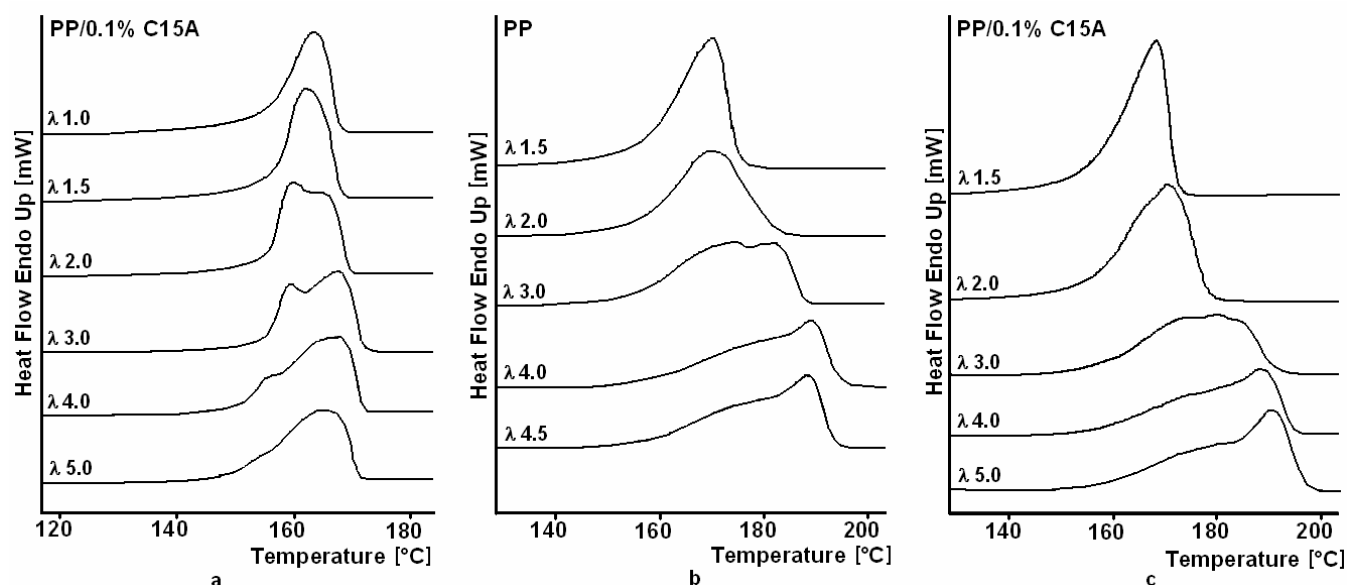


Figure 1 DSC-CM (a) and DSC-CLM (b, c) melting thermograms of PP and PP/0.1%C15A composite fibres in dependence on draw ratio

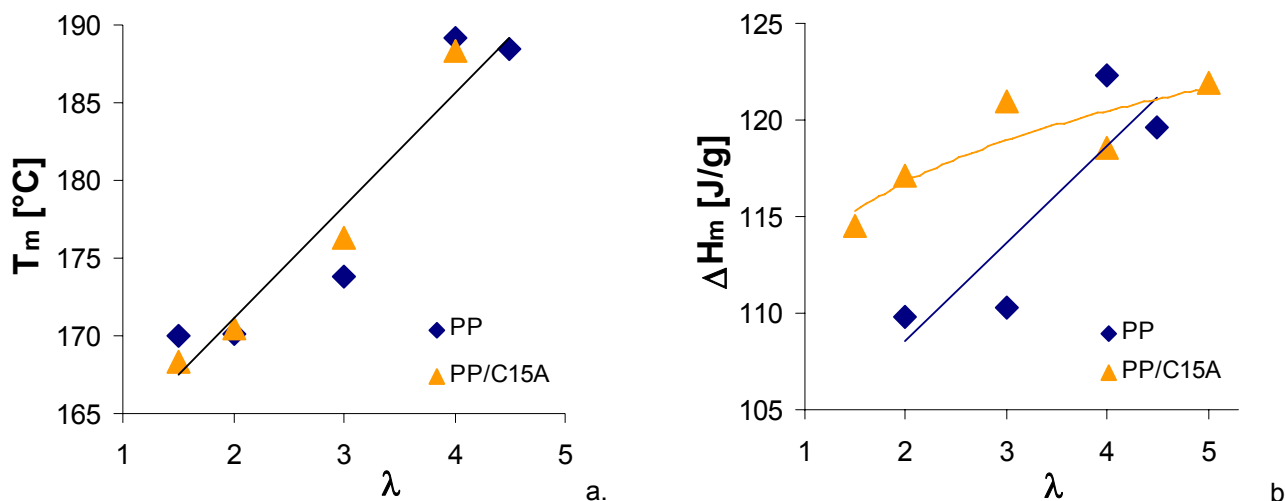


Figure 2 DSC-CLM melting temperature T_m (a) and melting enthalpy ΔH_m (b) versus draw ratio of PP composite fibres

Generally, DSC-CLM method provides the higher melting enthalpy for PP/organoclay fibers (higher crystallinity) in contrast to DSC-CM method, particularly for lower draw ratio. The effect of organoclay concentration on melting temperatures T_m is illustrated in Figure 3a. Melting temperature passes through a slight maximum at 0.02-0.1 wt% of organoclay and decreases at higher concentration of nanoparticles. Decrease of melting temperature of oriented fibers obtained by DSC CLM method is

proportional to decrease of orientation of non-crystalline phase, approximately also average orientation. Decrease of melting temperature (DSC CLM method) does not depend on orientation of crystalline phase. The dependence of enthalpy (crystallinity) on organoclay concentration passes through clear maximum at 0.1 wt.% and practically does not change with the presence of compatibiliser-dispersant (Figure 3b).

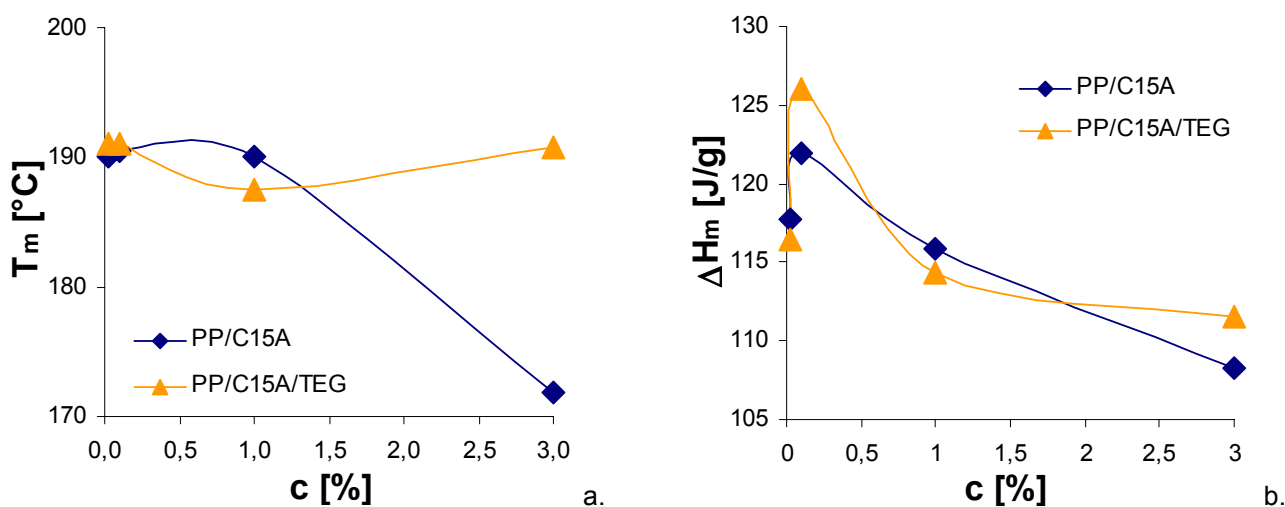


Figure 3 DSC-CLM melting temperatures T_m (a) and melting enthalpy ΔH_m (b) versus concentration of organoclay in the PP fibres

3.2 WAXS and SAXS measurements

The total crystallinity of the oriented PP matrix of fibers consists of the fraction of α -form modification X_α and fraction of mesophase X_m (Table 1).

On the basis of WAXS measurements the maximum total crystallinity was found for low concentration of organoclays, and at the same time for maximum draw ratio.

Results are consistent with these obtained from DSC-CLM method. With higher concentration of C15A organoclay the total crystallinity of the PP matrix gradually decreases mainly due to significant decrease of the mesophase fraction X_m . The higher content of α -modification was found for drawn fibers and for higher content of C15A organoclay. The sizes of α -form crystallites decrease gradually for lower draw ratio and higher concentration of C15A organoclay in PP matrix.

SAXS measurement was used for evaluation of d-spacing between silicate layers in the C15A and C30B organoclays (Figures 4, 5).

Three characteristic intensity peaks were found for pure C15A organoclay corresponding with d-spacing of 3.5, 2.0 and 1.3 nm, respectively and one peak for C30B organoclay corresponding with 1.9 nm distance between layers of silicate. Only single characteristic peak for C15A

organoclay, corresponding with $d=2.0$ nm, in the PP fibers appeared for higher concentration (1-3 wt.%) and for lower draw ratio (λ_1, λ_3). The peak for C15A in PP fibers is weak and broad. It could not be resolved for high draw ratio and lower concentration (0.02-0.1%), (Figures 4b, 5a).

The results show that cold drawing of the fibers contributes to intercalation and exfoliation of C15A organoclay in the matrix of PP fibers. The intercalated and exfoliated fraction of organoclay grows for the lower concentration of organoclay and high draw ratio.

The d-spacing of C30B in the PP fibers are clearly lower by 0.4 nm compared to pure C30B powder. Only for PP/C30B (1.0% + TEG) fibers at λ_{max} the intensity peak is slightly shifted towards smaller angles (larger distance) in comparison with composites without TEG compatibiliser-dispersant. The intensity peaks of other samples remained at the same position (Figure 5b). However, the difference is very minute. Based on SAXS results the d-spacing of C30B collapsed and layers distance decreased from 1.9 to 1.5 nm. The organic phase partially removes from the layers space in the PP matrix. This phenomenon is not rare for layered silicates and was presented also in other papers.

Table 1 Results of WAXS measurements of PP/organoclay composite fibers

Composition of fibers	Draw ratio λ	Total crystallinity X_c	Fraction of α form X_α	Fraction of mesophase X_m	Sizes of crystallites of α form $D_{(110)}$ [nm]	Sizes of mesophase crystallites [nm]
PP	3.0	0.621	0.338	0.283	6.5	3.4
PP	4.5*	0.625	0.311	0.314	5.4	3.1
PP/1.0% C15A	1.0	0.620	0.272	0.348	8.4	3.3
PP/1.0% C15A	3.0	0.668	0.407	0.261	7.1	3.4
PP/0.02% C15A	5.0*	0.714	0.338	0.376	6.2	2.7
PP/0.1% C15A	5.0*	0.688	0.347	0.341	4.6	2.8
PP/1.0% C15A	4.5*	0.627	0.311	0.316	7.0	3.1
PP/3.0% C15A	3.0*	0.571	0.388	0.183	11.6	3.5
PP/1.0% C30B	3.0	0.616	0.409	0.207	7.7	3.7
PP/1.0% C30B	4.5*	0.658	0.389	0.269	6.3	3.1
PP/1.0% C30B/TEG	3.0	0.636	0.396	0.240	6.6	3.8
PP/1.0% C30B/TEG	4.5*	0.636	0.435	0.201	5.2	4.0

* maximal draw ratio

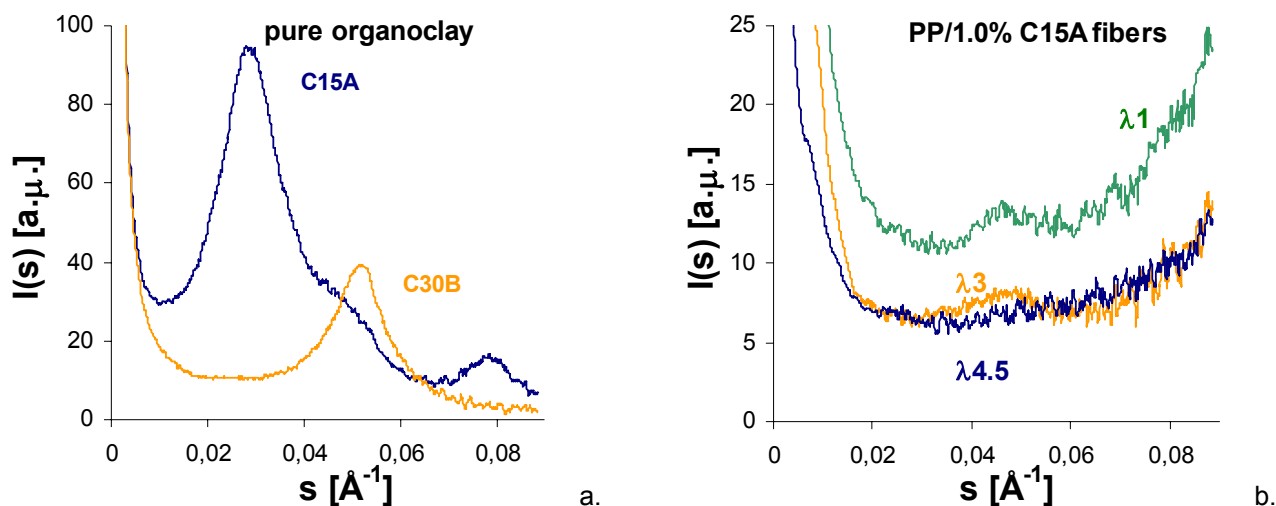


Figure 4 SAXS curves for evaluation the d-spacing of pure organoclay (a) and PP/organoclay C15A 1.0 wt.% composite fibres (b). Slit-smearred data after Lorentz correction

The SAXS results have shown that d-spacing of C15A organoclay in PP fibers grows during spinning and drawing mainly at low concentration and maximum draw ratio. In contrast, no positive change regarding to intercalation and exfoliation of C30B organoclay was observed.

In the case of C15A organoclays the higher amount of alkyl ammonium ion and higher compatibility of hybrid particles with PP enables the diffusion of polymer chains into galleries of the silicates and consequently forming of the uniform composite morphology.

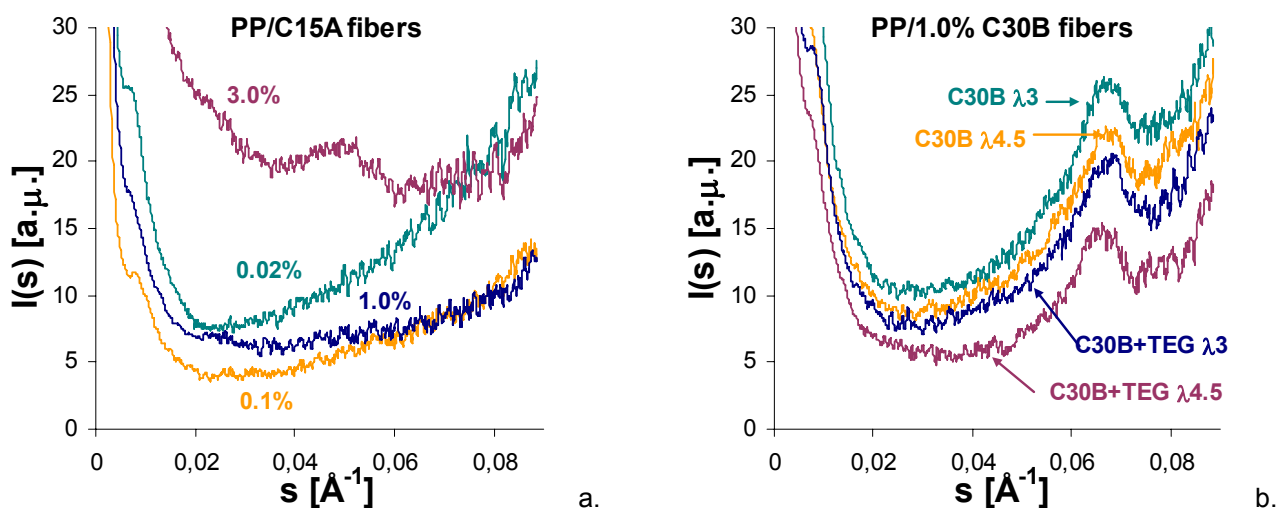


Figure 5 SAXS curves for evaluation the d-spacing of PP/organoclay composite fibres in dependence on concentration of C15A for λ_{max} (a) and draw ratio of PP/C30B 1.0 wt.% fibres (b). Slit-smearred data after Lorentz correction

3.3 Sonic average orientation of the fibers

Analysis of the average orientation f_{α} carried out using sonic velocity method shows an effect of organoclay on orientation of structure elements in the PP matrix of the PP/organoclay fibers (Table 2).

The positive effect of organoclay C15A and C30B was found for maximum draw ratio (λ_{max}) for concentration of organoclays about 0.1 wt.%. Higher content of organoclays leads to decrease of orientation of fibers at constant draw ratio (λ_3) but also at maximum draw ratio (λ_{max}).

The higher average orientation was obtained for PP/C15A compared to PP/C30B fibers. Compatibiliser–dispersant S44P contributes to higher orientation of PP/C15A fibers and TEG compatibiliser facilitates orientation of both PP/C15A and PP/C30B fibers. The results of orientation of the fibers correspond with these obtained by DSC-CLM method and with mechanical properties of fibers. The effect of MMT at low concentration and absence of continuous phase of solid particles on sonic velocity of composite fibers was considered as negligible.

3.4 Mechanical properties

Both organoclays positively affect the tenacity and Young's modulus of PP composite fibers only at a low concentration, up to 1.0 wt% (Tables 3, 4).

A lower tenacity was found for PP fibers containing C30B without compatibiliser and with S44P one. Analysis of the mechanical properties of fibers shows predominant effect of supermolecular structure and orientation of fibers on both tenacity and Young's modulus (Tables 2-4, Figure 6). The orientation of fibers results from the deformation of fibers in drawing. The positive effect of low concentration of organoclay and compatibilisers on mechanical properties of PP composite fibers resides in the favourable deformation during the drawing process. The higher λ_{max} at drawing of fibers was achieved in this case.

From the thermal properties of PP composite fibers it can be concluded that while the melting temperature T_m , obtained using DSC-CM method for PP composite fibers weakly increases with the draw ratio, passes through broad maximum, the T_m obtained by DSC-CLM method, grows proportionally to the draw ratio (Figure 1b, 2a).

Table 2 Average orientation f_{α} of the PP/C15A and PP/C30B drawn composite fibers (λ_3 and λ_{max}), the content of compatibiliser is 40 wt.% related to the organoclay content

Composition of fibers	Content of organoclay [%]	f_{α} of PP/C15A fibers		f_{α} of PP/C30B fibers	
		λ_3	λ_{max}	λ_3	λ_{max}
PP	-	0.64	0.72	0.64	0.72
PP/OC	0.02	0.64	0.76	0.62	0.74
	0.1	0.63	0.76	0.66	0.75
	1.0	0.62	0.70	0.61	0.73
	3.0	0.53	0.64	-	-
PP/OC/S44P	0.02	0.64	0.75	0.59	0.69
	0.1	0.63	0.76	0.64	0.75
	1.0	0.64	0.71	0.63	0.69
	3.0	0.61	0.70	0.34	0.54
PP/OC/TEG	0.02	0.64	0.76	0.63	0.74
	0.1	0.63	0.75	0.62	0.73
	1.0	0.62	0.72	0.64	0.72
	3.0	0.60	0.71	0.50	0.62

Table 3 Tenacity σ , elongation at break ε and Young's modulus E of PP/C15A nanocomposite fibers

Composition of fibers	C _{OC} , [wt%]	Draw ratio, λ_{max}	σ [cN/tex]	ε [%]	E [N/tex]
PP	-	4.5	41.6 ± 0.7	33.8 ± 4.1	4.73 ± 0.17
PP/C15A	0.02	5	54.2 ± 3.5	27.7 ± 4.1	4.89 ± 0.25
	0.1	5	55.0 ± 1.9	25.6 ± 2.0	4.54 ± 0.42
	1.0	4.5	41.7 ± 2.4	36.1 ± 5.6	4.30 ± 0.28
	3.0	3	24.3 ± 0.8	98.5 ± 7.9	2.34 ± 0.08
PP/C15A/S44P	0.02	5	51.7 ± 2.9	27.2 ± 4.4	4.65 ± 0.30
	0.1	5	53.1 ± 1.0	26.0 ± 1.3	4.57 ± 0.26
	1.0	4.5	43.2 ± 1.8	34.2 ± 9.4	4.58 ± 0.24
	3.0	3	38.3 ± 2.0	41.0 ± 12.4	3.76 ± 0.16
PP/C15A/TEG	0.02	5	52.2 ± 1.9	25.3 ± 2.0	4.92 ± 0.16
	0.1	5	51.4 ± 1.3	24.1 ± 1.6	4.99 ± 0.11
	1.0	4.5	43.8 ± 1.4	44.7 ± 14.2	4.75 ± 0.23
	3.0	3	45.8 ± 2.9	25.8 ± 4.0	4.46 ± 0.17

Table 4 Tenacity σ , elongation at break ε and Young's modulus E of PP/C30B nanocomposite fibers

Composition of fibers	C _{OC} , (wt%)	Draw ratio, λ_{max}	σ [cN/tex]	ε [%]	E [N/tex]
PP	-	4.5	41.6 ± 0.7	33.8 ± 4.1	4.73 ± 0.17
PP/C30B	0.02	5	52.5 ± 1.9	29.4 ± 4.0	4.99 ± 0.19
	0.1	4.5	49.4 ± 2.3	27.2 ± 3.3	4.83 ± 0.16
	1.0	4.5	43.9 ± 1.6	20.3 ± 1.3	4.78 ± 0.18
	3.0	-	-	-	-
PP/C30B/S44P	0.02	5	44.4 ± 1.7	43.4 ± 11.9	4.56 ± 0.16
	0.1	5	56.7 ± 0.8	24.6 ± 1.7	5.38 ± 0.14
	1.0	4.5	38.1 ± 3.4	24.7 ± 6.2	4.57 ± 0.27
	3.0	3	12.3 ± 0.7	58.5 ± 13.3	1.49 ± 0.10
PP/C30B/TEG	0.02	5	56.3 ± 0.8	25.2 ± 1.0	5.31 ± 0.22
	0.1	5	55.1 ± 0.9	26.0 ± 1.4	4.73 ± 0.35
	1.0	4.5	44.0 ± 2.4	28.3 ± 3.2	4.68 ± 0.18
	3.0	3	22.4 ± 1.5	81.8 ± 11.2	2.25 ± 0.14

Analysis of these dependences and tensile properties of composite fibers shows proportionality between the tenacity of fibers and melting temperatures T_m (Figure 6a). The highest T_m temperature corresponds with the highest tenacity and modulus of the fibers at the maximum draw ratio λ_{max} within the 0.02-0.1 wt% concentration of organoclay in PP fibers.

The melting enthalpy ΔH_m obtained by DSC-CLM methods increase with draw ratio of the fibers. Sharp maximum of the melting enthalpy at 0.02-0.1 wt% of C15A (Figure 2b)

unambiguously corresponds with the highest values of tensile properties of PP composite fibers (Figure 6b).

With regard to results obtained, the higher tensile properties of PP/organoclay composite fibers correspond with higher total crystallinity and to finer supermolecular structure, e.g. lower size of α -form crystallites. In addition, the lower content of mesophase crystallites has a positive effect on the tensile properties of fibers (Tables 1, 3 and 4).

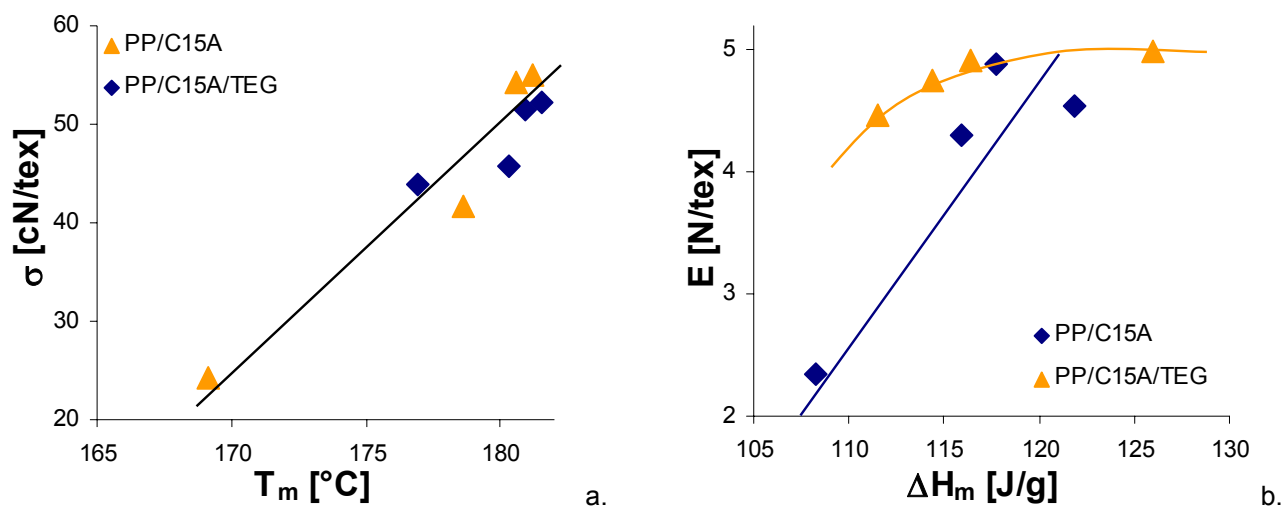


Figure 6 Dependence of the tenacity σ versus melting temperature T_m (a) and Young's modulus E versus melting enthalpy ΔH_m (b) (DSC-CLM) of PP/C15A composite fibres

The WAXS analysis of the PP composite fibers provides the results corresponding with DSC-CLM measurement. The higher tensile properties of PP composite fibers correspond with higher crystallinity (melting enthalpy), (Table 1, Figures 3b and 6b), orientation of amorphous region – higher T_m (Figure 6a), higher average orientation (Table 2), higher α -form fraction and lower size of both α -form and mesophase crystallites (Table 1).

4 CONCLUSIONS

The analysis of the thermal properties, supermolecular structure, orientation and mechanical properties of PP/organoclay composite fibers obtained in the experimental work allow to draw the following conclusions:

- Tenacity and Young's modulus of the PP/organoclay composite fibers correspond with their DSC-CLM melting temperature (orientation of non-crystalline regions) and melting enthalpy (total crystallinity). The higher melting temperature T_m and melting enthalpy ΔH_m , the higher tenacity and modulus of fibers.
- Tenacity and Young's modulus of PP/organoclay fibers increase gradually with higher total crystallinity obtained by WAXS method, higher α -form fraction, lower fraction of mesophase crystallites

and lower size of both the α -form and mesophase crystallites. These parameters were found for PP/organoclay composite fibers containing 0.02-1.0 wt% of organoclay C15A (C30B with TEG dispersant, only).

- DSC-CLM method is suitable for the evaluation of thermal properties of the drawn PP and PP/organoclay composite fibers. This method is more sensitive for oriented polymers in comparison with conventional DSC measurements.

Acknowledgment: This work was supported by EC, FP6 Project: NMP3-CT-2005-516972 and Slovak Research and Development Agency under contract No. VMSP-P-0007-09.

5 REFERENCES

1. Wang K., Xiao Y., Na B., Tan H., Zhang Q., Fu Q.: Shear amplification and re-crystallization of isotactic polypropylene from an oriented melt in presence of oriented clay platelets, *Polymer* 46(21), 2005, 9022-9032
2. Ma J., Zhang S., Qi Z., Li G., Hu Y.: Crystallization behaviors of polypropylene/ montmorillonite nanocomposite, *J App Polym Sci* 83(9), 2002, 1978-1985
3. Zhang Q.X., Yu Z.Z., Yang M., Ma J., Mai Y.W.: Multiple melting and crystallization of nylon-66/montmorillonite nanocomposites, *J Polym Sci, Part B: Polymer Physic* 41(22), 2003, 2861-2869

4. Maiti P., Nam P.H., Okamoto M., Hasegawa N., Usuki A.: Influence of Crystallization on Intercalation, Morphology, and Mechanical Properties of Polypropylene/Clay Nanocomposites, *Macromolecules* 35(6), 2002, 2042-2049
5. Somwangthanaroj A., Lee E.C., Solomon M.J.: Early Stage Quiescent and Flow-Induced Crystallization of Intercalated Polypropylene Nanocomposites by Time-Resolved Light Scattering, *Macromolecules* 36(7), 2003, 2333-2342
6. Nowacki R., Monasse B., Piorkowska E., Galeski A., Handin J.M.: Spherulite nucleation in isotactic polypropylene based nanocomposites with montmorillonite under shear, *Polymer* 45(14), 2004, 4877-4892
7. Choi W.J., Kim S.Ch.: Effects of talc orientation and non-isothermal crystallization rate on crystal orientation of polypropylene in injection-molded polypropylene/ethylene-propylene rubber/talc blends, *Polymer* 45(7), 2004, 2393-2401
8. Hambir S., Bulakh N., Jog J.P.: Polypropylene/Clay nanocomposites: Effect of compatibilizer on the thermal, crystallization and dynamic mechanical behaviour, *Polym. Eng. Sci.* 42(9), 2002, 1800-1807
9. Peterlin A.: Molecular model of drawing polyethylene and polypropylene, *J. Mater. Sci.* 6(6), 1971, 490-508
10. Chatterjee A., Deopura B.L.: High modulus and high strength PP nanocomposite filament, *Composites, Part A* 37(5), 2006, 813-817
11. Tomio K., Seiichi M.: Preparation of easily dyeable polyethylene terephthalate fiber, JP57161120, 1982
12. Young R.J., Eichhorn S.J.: Deformation mechanisms in polymer fibres and nanocomposites, *Polymer* 48(1), 2007, 2-18
13. Young R.J.: Monitoring Deformation Processes in High-performance Fibres using Raman Spectroscopy, *J. Text. Inst.* 86(2), 1995, 360-381
14. Grebowicz J.S., Brown H., Chuah H., Olvera J.M., Wasiak A., Sajkiewicz P., Ziabicki A.: Deformation of undrawn poly(trimethylene terephthalate) (PTT) fibers, *Polymer* 42(16), 2001, 7153-7160
15. Lyon R.E., Farris R.J., MacKnight W.J.: A differential scanning calorimetry method for determining strain-induced crystallization in elastomeric fibers, *J. Polym. Sci. Polym. Lett. Ed.* 21(5), 1983, 323-328
16. Marcinčin A., Hricová M., Marcinčin K., Hoferíková A.: Spinning of Polypropylene /Organoclay Composites, Thermal and Mechanical Properties of Fibres, *Tekstil: Časopis za tekstilnu tehniku i konfekciju* 57(4), 2008, 141-148
17. Marcinčin A., Hricová M., Marcinčin K., Hoferíková A.: Study of Rheological, Thermal and Mechanical Properties of Polypropylene/ Organoclay Composites and Fibres, *Fibres and Textiles in EE* 17(6), 2009, 22-28
18. Rabiej M.: Determination of the degree of crystallinity of semicrystalline polymers by means of the „OptiFit” komputer software, *Polimery* 47, 2002, 423

POLYPROPYLEN/ORGANOÍLOVÉ KOMPOZITNÉ VLÁKNA, ŠTRUKTÚRA, TERMICKÉ A MECHANICKÉ VLASTNOSTI

Translation of the article

Polypropylene/organoclay composite fibers, structure, thermal and mechanical properties

V tomto príspevku je prezentovaný vplyv jednosmernej deformácie PP/organoílových kompozitných vlákien pri zvlákňovaní a dlžení na ich nadmolekulovú štruktúru ako aj termické a mechanické vlastnosti. Ako anorganické plnivá boli v práci použité komerčné typy organoílov Cloisit C15A a Cloisit C30B, obidva na báze montmorilonitu. Nadmolekulová štruktúra bola hodnotená pomocou DCS analýzy a metódy difrakcie X-lúčov. DCS merania boli stanovené konvenčnou metódou (CM) a metódou konštantnej dĺžky (CLM), pri ktorej je počas celého merania zaistená konštantná dĺžka vzorky vlákna. Priemerná orientácia vlákien bola stanovená metódou rýchlosti zvuku. Na stanovenie interkalácie polypropylenu v medzivrstvových galériách organoílov bola použitá metóda SAXS. Pevnosť a Youngov modul kompozitných vlákien boli hodnotené v závislosti na termických vlastnostiach a nadmolekulovej štruktúre, ako aj v závislosti na interkalácii a exfoliacii (nano)plnív v polymérnej matrici.

BLENDED TEXTILES WITH FIBERS PROTEX-M FOR EXTREME CONDITIONS

M. Nejedlá

*Technical University of Liberec, Faculty of Textile Engineering, Department of Clothing technology, Studentská 2, 461 17 Liberec, Czech Republic
marie.nejedla@tul.cz*

Abstract: *This article focuses on the verification of properties of blended textiles with Protex-M fibers. The method allows the assessment of the behavior of textiles during short-term contact with a flame. Flame retardation has been demonstrated for selected textiles (single-layer knitted, single-layer woven and sandwich layers) without side effects, which is a beneficial situation for the use of blended textiles in contact with a living organism especially in emergency situations, that is, clothing for firefighters. Multilayer sandwich blended textiles with Protex-M fibers significantly increased flame-damage resistance.*

Key words: *Modacrylics, Protex-M fibers, blended textiles for emergency clothing, for firefighters.*

1 INTRODUCTION

Nowadays, there is a large range of clothing and accessories on the market to protect the human body in extreme conditions, such as fire and heat. Materials with a limiting oxygen index (LOI) up to 21 are usually considered flammable. Polymers with aromatic compounds, for example, those containing halogens, aramides and modacrylics have a lower flammability. All inorganic glass and ceramic fibers are practically non-flammable. Materials which only melt in a flame are also sometimes considered non-flammable and are immediately extinguished after removal from a flame, for example PVC or oxidized acrylics.

Special flame-resistant protective clothes create a primary barrier ensuring reliable and permanent protection. Non-flammable underclothing acts as a secondary heat barrier and ensures the necessary physiological comfort.

Protex-M modacrylic fibers exhibit characteristics which increase protection of the body. Thanks to their molecular structure and properties, the risk of melting is not a threat as it is in synthetic thermoplastic materials. This is enforced everywhere where danger caused by fire and heat exists.

2 CHARACTERISTICS AND APPLICATION OF MODACRYLIC FIBERS

A modacrylic is a synthetic copolymer. Modacrylic fibers usually contain 50 to 80% acrylonitrile and 20 to 50% halogen-containing comonomer, such as vinylchloride or vinylidenechloride. Examples of modacrylic fibers are trademarked Dynel (acrylonitrile and polyvinyl chloride) and Verel (acrylonitrile and vinylidene chloride) [1].

Commercial production of modacrylic fibers began in 1949 by Union Carbide Corporation in the United States. In 1960 the Federal Trade Commission decided to separate above mentioned two types of fibers and establish separate categories for them. Current modacrylic fiber producers include Solutia Inc. in the U.S. and Kaneka Corporation in Japan (under the brand "Kanecaron") [2]. There are some suppliers in China, India and the United Kingdom as well. When the LOI reaches a value of 32-34, the material is classified as non-flammable. It is well-processed in the textile industry and can be mixed with cellulose fibers, such as wool, cotton, polyester, and silk [3].

Modacrylic Protex-M is a material which inherently slows down burning – it is flame retardant (FR). It has a unique structure as

shown in the cross-section of Figure 1, which lends softness to it. This is good for underclothing which needs to look natural and feel comfortable while being worn, particularly with the addition of natural fibers, such as cotton [4].

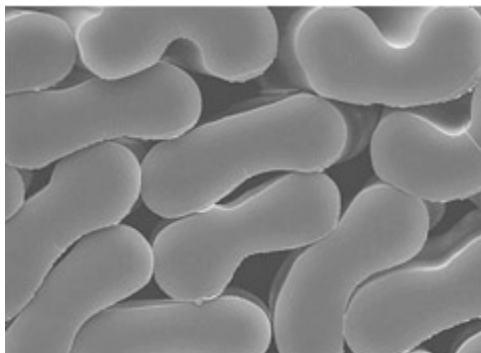


Figure 1 Cross-section of modacrylic fibers [4]

Protex-M modacrylic fibers are imported from Japan and then the yarn is spun using high quality cotton. They are produced on request in a mixture with 2% antistatic fibers, which are then woven and colored directly in the factory [3].

The flammability of a textile is measured according to the susceptibility of textile materials to ignite and their behavior while burning. Flammability is influenced by the physical (shrinkage, fusibility), chemical (C, O, etc., content), and geometric attributes of the material (shape, weight) [4].

Flammability, auto-ignition, and LOI classification and testing are some of the regular tests. LOI indicates the minimal concentration of oxygen in a defined mixture of nitrogen and oxygen in which the specimen will still burn [4].

Fire safety tests of the textile materials are performed on instruments for measuring LOI as shown in Figure 2 [5].

The test method is based on the ASTM D-2863 norm established in the USA in 1977 [5, 6]. The examined specimen is put into the glass tube of the instrument from which comes a combination of oxygen and nitrogen, and is ignited from above. If the specimen burns for longer than 180 seconds or if the flame reaches a certain height in the tube, the test is repeated with a lower concentration of

oxygen. The test is performed until 50% of the specimen burns at a certain concentration [4].



Figure 2 LOI Measurement tool [5]

The % concentration is calculated according to the formula:

$$LOI = \frac{[O_2]}{[N_2] + [O_2]} 100[\%] \quad (1)$$

where O_2 means the oxygen volume and N_2 the nitrogen volume.

The higher the LOI value, the greater the resistance of the material against ignition and burning [4].

60% Protex-M/40% cotton blend has a higher LOI compared with 100% Protex-M sample. This progress is shown on graphs in Figure 3 [7].

Some of the main characteristics and requirements for products made from Protex-M modacrylic fibers are: resistance to burning, dyeing, modification, processing techniques, LOI, lightweight, strength, process-ability, heating insulation, resilience, maintenance, and comfort. Textiles containing these fibers are either non-flammable or have reduced flammability that persists even after frequent washing or extended use. Furthermore, they have self-extinguishing capabilities. Their lowered flammability is maintained even when modacrylic yarns are used in wefts, and standard cellulose or polyester yarns can be used. When lit, the fibers carbonize which forms an effective barrier that prevents the

fire from spreading. Modacrylic fibers can also increase the quality of processing and the quality of clothing by using flame retardant ingredients in the textiles.

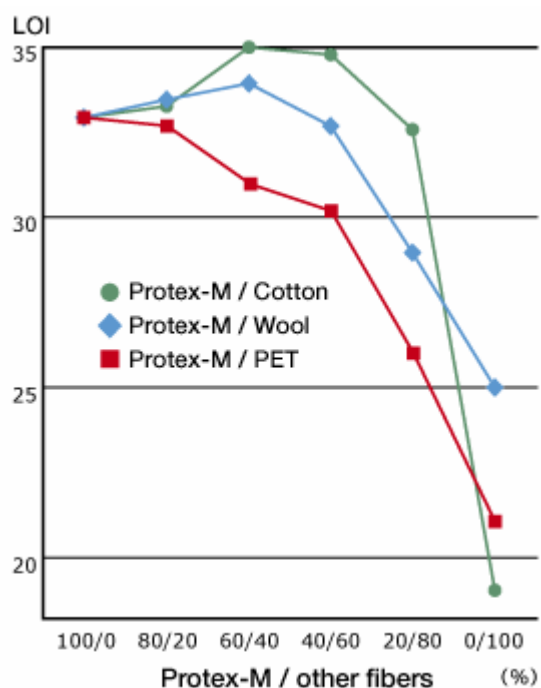


Figure 3 LOI values - Protex-M/ other fibers [7]

LOI values of selected fibers are shown in Figure 4 [7].

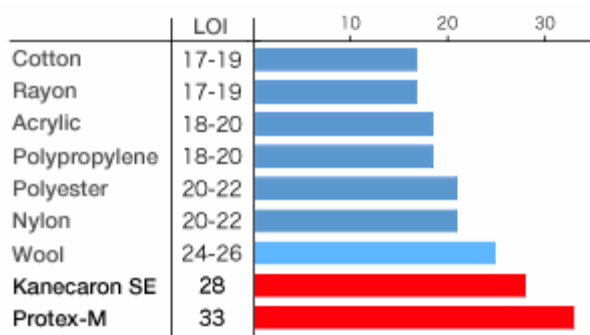


Figure 4 LOI values of selected fibers [7]

Textiles in combination with Protex-M fibers can be woven, knitted or non-woven, and have an unlimited amount of colorings. They can be colored by using basic cationic dyes; with antistatic modification; and also with modification against UV light. They are durable, resistant to chemicals and do not create toxic gases. They are easily

maintained, as they can be washed at temperatures from 70°C to 100°C, and exhibit minimal shrinkage and good color preservation and are also soft to the touch [7].

Protection against fire and heat is the most important protective priority to increase the safety of people.

The combination of protective clothing and non-flammable clothes guarantees the optimal protection of the human body exposed to extreme conditions, namely the effects of fire and heat. Their characteristics are permanent and the risk of melting is not a threat, as in other synthetic, thermoplastic fibers [3].

Protex-M fibers are used wherever there is danger of fire and heat:

- in the petrochemical industry for welding
- in foundries
- for work with molten metals
- in protection from heat and fire [3].

Protex-M fibers are designed in such a way that their characteristics perfectly match the characteristics of natural or artificial fibers for the production of textiles of the highest quality with an exceptional touch and appearance [7, 8].

It does not melt or form molten droplets which could burn the skin. Instead of a sooty layer, it forms a protective layer which is able to give the user more time to deal with dangerous areas.

By compounding grains in the weft material in the correct amount, Kanecaron has developed FR characteristics on other fibers so that the whole textile will be fire-resistant. In contrast to chemically treated textiles, FR Kanecaron has long lasting characteristics and is not influenced by attrition, frequent washing or chemical washing [7, 8].

3 EXPERIMENT

3.1 Materials

The experiment focuses on the verification of properties of blended textiles with Protex-M. The actual percentage of components (acrylonitrile-vinyl chloride or acrylonitrile-

vinylidenechloride) in the tested samples could not be established.

- The first textile material studied is a dual cuff knitted in dark blue, composed of 60% Protex-M/40% cotton, designed for the production of undergarments which protects the body from heat and fire.
- The second material is a textile with a twill-weave grey woven, composed of 54% Protex-M/44% cotton/2% Antistatico, designed for the production of outer protective clothing— such as jackets and pants, or jumpsuits also protecting the body in conditions of increased heat or fire. It is always used in combination with clothes protecting the body.

3.2 Methods of analysis

Both types of materials were subjected to testing according to the ČSN EN ISO 15025 norm. The method evaluates the characteristics of the textiles and their behavior during limited contact with a small flame under controlled conditions [9].



Figure 5 The SDL Atlas M233B AutoFlam tool - a) effects of a flame applied to the surface & b) effects of a flame applied to the edge

The materials were tested on the SDL Atlas M233B AutoFlam tool, Figure 5a, b, the type of gas used – propane butane, at a temperature of 21°C and 63% RH. The size of the specimen was 160x200 mm.

3.3 Materials testing

The tests were repeatedly performed by applying a flame to the surface and applying a flame to the edge of a knitted textile in the wale direction and the course direction as shown in Figure 6 and in case of a woven textile in the direction of warp and weft, Figure 7.

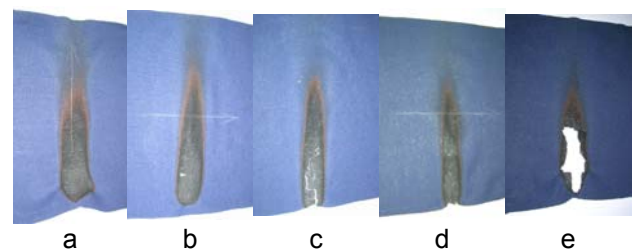


Figure 6 Image of examined knitted textile - **limited spreading of the flame: onto the surface** - a) in the direction of wale, b) in the direction of course, **onto the edge** – c) in the direction of wale, d) in the direction of course, e) example of burnt knitted textile crumbling

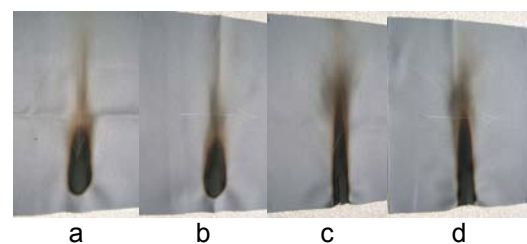


Figure 7 Image of examined woven textile - **limited spreading of the flame: onto the surface** – a) in the direction of a warp, b) in the direction of a weft, **onto the edge** – c) in the direction of a warp, d) in the direction of a weft

The tests were subsequently performed on **sandwiches** - that is, woven (primary) and knitted (secondary) layers, and the above-inspected materials were used. The upper woven textile was exposed from the front side to the effect of a flame onto the surface, Figure 8.

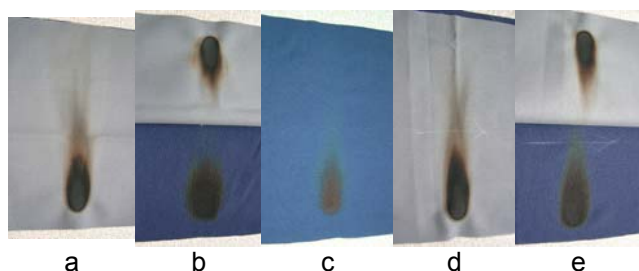


Figure 8 Image of the examined layer of the primary and secondary textiles – **limited spreading of the flame: to the surface** – a) the front side of the woven textile in the direction of the warp, b) back side of the woven textile in the direction of the warp and knitted textile of the direction of wale c) back side of the knitted textile in the direction of wale; d) the front side of a woven textile in the direction of a weft, e) back side of the woven textile in the direction of a weft and knitted textile of the direction of course

When tested with a flame applied to the edge, the flame affected both textiles simultaneously, Figure 9.

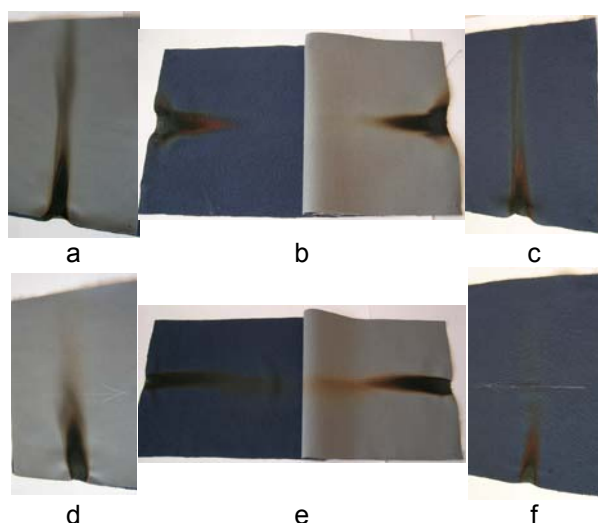


Figure 9 Image of the examined layer of the primary and secondary textiles – **limited spreading of the flame: to the surface** – a) the front side of the woven textile in the direction of the warp, b) back side of the knitted textile in the direction of the wale and woven textile of the direction of a warp c) the front side of the knitted textile in the direction of wale, d) the front side of a woven textile in the direction of a weft, e) back side of the knitted textile of the direction of course and woven textile of the direction of a weft, f) the front side of the knitted textile in the direction of course

4 RESULTS OF TESTS AND DISCUSSION

The results of the tests of the knitted (secondary) and woven (primary) layers used for the production of protective clothing during limited contact with a standard flame are given in Table 1.

Knitted Textile – during burning, smoke and a foul-smelling gas were given off. Within 10 seconds after removing the flame, the knitted textile stopped burning on its own. After the test, a burnt strip with the visible structure of the knitted textile was charred and brittle (it crumbled when bent). The photographs attached in Figure 6 show an image of the burning.

Woven Textile – during burning, smoke and a foul-smelling gas were simultaneously given off. After removing the flame for 10 seconds, the woven textile had already stopped burning. During the test, the edge of the woven textile burnt down with afterglow, without propagating into the body. On the woven textile there was a burnt strip with a visible structure, charred and brittle (it crumbled when bent). The photographs attached in Figure 7 show images of the burning. The results of the tests of knitted and woven textiles used in the primary and secondary layers of protective clothing during limited contact with a small flame are given in Table 2.

Burning of both layers (applied to the surface) – the flame was active for 10 seconds. After removing the flame, the layer did not continue to burn. After the test, a burnt line was visible on both layers with the visible structure of the textiles, though charred and brittle (it crumbled when bent).

Burning of both layers (applied to the edge) – the flame was active again for 10 seconds. After removing the flame, the layer itself did not continue to burn. During the test, the edge of the fabric burnt down with afterglow without propagating into the body. After the test, a burnt line was visible on both layers with the visible structure of the textile, though charred and brittle (it crumbled when bent).

Table 1 The results of the tests of limited contact with a small flame under controlled conditions - Knitted and Woven Textiles

Type of textiles	Knit				Woven			
	Orientation of best specimen				Orientation of best specimen			
	Onto the surface		The edges		Onto the surface		The edges	
Side-effects when tested	Column direction	Direction of the line	Column direction	Direction of the line	Direction warp	Direction weft	Direction warp	Direction weft
Duration of flaming [s]	0.0 *	0.0 *	0.0 *	0.0 *	0.0 *	0.0 *	0.0 *	0.0 *
Duration of afterglow [s]	0.0 *	0.0 *	0.0 *	0.0 *	0.0 *	0.0 *	20	25
Flaming debris	0	0	0	0	0	0	0	0
Debris	0	0	0	0	0	0	0	0
Max. extent of hole [mm]	0	0	0	0	0	0	0	0
Flaming to edge	0.0 **	0.0 **	0.0 **	0.0 **	0.0 **	0.0 **	0.0 **	0.0 **
Max. damaged length [mm]	0	0	0	0	0	0	0	0

* Values in the table were close to zero. It depends on the speed of stopping timer.

** Immediately after approaching the burner, the textile began to burn (probably one of the components) in the portion above the flame.

Table 2 The results of the tests of limited contact with a small flame under controlled conditions – sandwich – woven (primary) and knitted (secondary) textiles

Type of textiles	Knit + Woven			
	Orientation of best specimen			
	Onto the surface		The edges	
Side-effects when tested	Column direction	Direction of the line	Column direction	Direction of the line
	/	/	/	/
	Direction warp	Direction weft	Direction warp	Direction weft
Duration of flaming [s]	0.0 *	0.0 *	0.0 *	0.0 *
Duration of afterglow [s]	0.0 *	0.0 *	25	25
Flaming debris	0	0	0	0
Debris	0	0	0	0
Max. extent of hole [mm]	0	0	0	0
Flaming to edge	0.0 **	0.0 **	0.0 **	0.0 **
Max. damaged length [mm]	0	0	0	0

* Values in the table were close to zero. It depends on the speed of stopping timer.

** Immediately after approaching the burner, the textile began to burn (probably one of the components) in the portion above the flame.

5 CONCLUSION

The results suggest that the single-layer and sandwich blended textiles prevent the spread of flame and show no sign of melting or dripping. The sandwich layer is identified by the after-burning flame-glow without spreading to the surfaces. The affected part clearly exhibits pyrolysis (charring) of the polyacrylonitrile fibers simultaneously with evidence of vaporization, thereby reducing the size of the pores of the textile and so completely stopping the burning.

Increases in the duration of afterglow are caused by:

- a higher percentage of cotton fibers in the textile,
- the direction from which the flame is applied - flame acting on the front and reverse side,
- a momentary delay in recording the end time of the test,
- an increase in the thickness of the textile.

The duration of the afterglow is also dependent on the type and structure of the textile, for example, if it is woven, the afterglow lasts longer.

The affected areas of both researched blended textiles were charred. Test images

show the intensity of the charred areas. Single-layer (knitted) textiles designed for the secondary layer is rubbed off during handling. Textiles (woven) single-layer intended for the primary layer are in tact, but damaged areas occur when folded or after frequent handling. The sandwich-layered, blended textiles flame-affected areas were also charred. The burnt primary part of the sample (woven) breaks during folding and handling whereas the burnt secondary layer (knitted) remains in tact and the coherence of textile is not diminished.

Tests have shown that damage occurs, especially in the primary (upper) layer. In addition, the sandwich layer can be multi-layered, that is, interlining and lining textiles produced from mixtures also containing Protex-M. Multilayer sandwich textiles increase flame-damage resistance. The researched blended textiles fulfil all the prerequisites to allow someone enough time to get to a safe environment. The requirements regarding the combustible

properties of textiles that are designed to protect the body from exposure to fire and heat are specified in the Government NV 21/2003 Coll. It sets out the technical requirements for personal protective equipment.

6 REFERENCES

1. <http://www.britannica.com/EBchecked/topic/468259/polyacrylonitrile-PAN>
2. <http://en.wikipedia.org/wiki/Modacrylic>
3. <http://www.alibaba.com/showroom/protex-m.html>
4. http://cs.wikipedia.org/wiki/Hořlavost_textilíí
5. <http://www.astm.org>
6. ASTM D-2863. Standard Test Method for Measuring the Minimum Oxygen Concentration to Support Candle-Like Combustion of Plastics. (Oxygen Index).
7. <http://www.kanecaron.com/whats/index.html>
8. <http://www.waxmanint.co.uk/kanecaron.html>
9. ČSN EN ISO 15025. Ochranné oděvy – Ochrana proti teplu a ohni – Metoda zkoušení pro omezené šíření plamene. (Protective Clothing – Protection against Heat and Fire – Method of Testing for the Limited Spreading of a Flame.)

SMĚSOVÉ TEXTILIE S VLÁKNY PROTEX-M PRO EXTRÉMNÍ PODMÍNKY

Translation of the article

Blended textiles with fibers Protex-M for extreme conditions

Článek je zaměřen na ověření vlastností směsových textilií s vlákny Protex-M. Uvedená metoda umožňuje zhodnocení chování textilií při krátkodobém kontaktu s plamenem. Na vybraných jednovrstvých a sendvičově vrstvených směsových textiliích bylo prokázáno zpomalení hoření bez vedlejších účinků, což je příznivá situace pro využití těchto směsových textilií v kontaktu s živým organismem, zvláště v nouzových situacích, tj. pro oděvy pro hasiče. Zkoušky textilií v sendviči prokázaly, že k poškození dochází, ale především u primární (vrchní) vrstvy. Kromě toho sendvičové textilie mohou být ještě v kombinaci s vložkovou a podšívkovou textilií vyráběných rovněž ze směsových textilií obsahujících Protex-M. Výrazně lepší nehořlavé vlastnosti vykazují sendvičově vrstvené směsové textilie, které tak dávají veškeré předpoklady k tomu, aby člověk získal dostatek času a dostal se do bezpečného prostředí.

ANALYSIS OF COTTON BLENDED YARNS IRREGULARITY

E. Moučková, P. Ursíny and P. Jirásková

*Technical University of Liberec, Faculty of Textile Engineering, Department of Textile Technologies, Studentská 2, 461 17 Liberec 1, Czech Republic
eva.mouckova@tul.cz; petr.ursiny@tul.cz; petra.jiraskova@tul.cz*

Abstract: *The paper is focused on the analysis of irregularity of combed yarns made from various blending ratios of CO/PL. The level of irregularity (CV) is evaluated in relation to the percentage representation of cotton in a yarn. Yarn irregularity is measured by a capacitive method (the apparatus Uster Tester IV-SX) and simultaneously by an optical method (the device QQM-3). The results showed a statistically significant effect of percentage representation of cotton in the yarn on both type of CV of yarn on short cut lengths. To clarify the obtained results of mass irregularity, the limiting yarn irregularity is analyzed in the relation to the parameters of raw material and yarn count. Concurrently, the modulus of relative transfer function of drafting mechanism is applied. The results of capacitive and optical measurement methods are compared too.*

Keywords: *Yarn irregularity, limiting mass irregularity, CO/PL blended yarn, Uster Tester, QQM-3, modulus of relative transfer function.*

1 INTRODUCTION

Yarn unevenness is one of the basic properties according to them yarn quality is assessed. The so-called mass irregularity is the most frequently measured and evaluated unevenness considering technological process of yarn production. It is defined as a variation of fibre mass in the cross-section or in the certain longitudinal sections (cut length) of fibrous product. It is influenced by used raw material, called own irregularity of fibres, i.e. variability in fibre diameters or in fibre cross-section and by technology of yarn production (arrangement of fibres in the yarn, faults in the technology, for example, incorrect setting of drafting mechanism, mechanical faults – misalign roller, spindle, etc.). Mass irregularity is measured by a capacitive method, which is employed, for example, by the apparatus Uster Tester, Keissoki evenness tester. Next currently important unevenness is a volume irregularity, where a variation of yarn diameter is measured optically by various methods regardless of its mass. The fluctuation in yarn diameter can be influenced, besides other, by variations of yarn twist. Representative methods of optical measurement of irregularity include, for

example, the devices QQM-3 [1], Zweigle Oasys [2], Keissoki laser spot [3] or CTT Lawson Hemphill - system YAS [4]. The instrument Uster Tester can be accessorized with optical sensors for yarn hairiness and yarn diameter testing too. Along with unevenness, the yarn faults are usually measured by these devices. Pneumatic or mechanical methods belong between other methods for measurement of irregularity of longitudinal fibrous product. They are used especially as a part of mass irregularity leveller on the carding or drawing machines.

Yarn mass irregularity affects variability of other properties of both yarn (for example twist, strength) and flat textiles (appearance, permeability, etc.) [5, 6]. The yarn volume (diameter) fluctuation also participates in the variability of the fabrics appearance.

Irregularity can be expressed by so called parameters and characteristic functions. The most commonly used parameters are quadratic unevenness CV, i.e. coefficient of variation of mass/diameter of the fibrous product reflecting the irregularity level.

As demonstrated by the number of works, e.g. [7], and the experience of experts from industry, the cause of the occurrence of higher mass irregularity (i.e. usually fault in the technological process of yarn production)

can be identified by characteristic functions (mostly spectrogram, length variation curve). The level of irregularity and other selected properties of produced longitudinal fibrous assembly can be compared with USTER®STATISTICS [8]. It is tables and graphs indicating the worldwide established quality reference values of fibrous product. The level of mass unevenness can possibly be compared with the calculated limiting mass irregularity.

In this work, the influence of blending ratio of CO/PL on combed yarn irregularity is analyzed. Yarn irregularity is measured simultaneously by both capacitive (the instrument Uster Tester IV-SX) and optical method (the device QQM-3). The limiting mass irregularity and the modulus of relative transfer function are applied for the analysis of mass irregularity results. The CV values from both instruments are compared.

2 USED PRINCIPLES OF YARN IRREGULARITY MEASUREMENT

2.1 Uster Tester IV-SX

On the apparatus Uster Tester IV-SX, irregularity and yarn faults is measured by capacitive measuring sensors. A high-frequency electric field is generated in the sensor slot between a pair of capacitor plates. If the mass between the capacitor plates changes, the electric signal is altered and the output signal of sensor changes accordingly. The result is an electric signal variation proportional to the mass variation of the test material passing through. This signal is then converted into digital signal [9]. This type of device measures the variability in longitudinal sections of min. 10 mm.

2.2 Device QQM-3

The device QQM-3 is an indicator of yarn quality developed in the Cotton Research Institute (VUB), Czech Republic. It is a portable device (Figure 1), which provides measurement of yarn and analysis of variation coefficient CV_{opt} of yarn diameter and measurement of yarn faults. The device is based on the optical principle. It has 2

optical sensors of 2 mm width, equipped with infra diodes and transistors positioned in the direction of yarn delivery, 10 mm apart. Sensors are programmed for sampling each 2 mm. Maximum measuring speed is 300 m/min [1].



Figure 1 Device QQM-3 [1]

2.3 Limiting mass irregularity of blended yarn

Limiting mass irregularity is the minimum possible unevenness caused by random fluctuation in the number of fibres in the product cross-section and by own irregularity of fibres. Calculations of limiting mass irregularity of blended fibrous product are based on the theory of random functions and use the assumption that the total variance is equal to the sum of individual variances under the conditions of their statistical independence:

$$\sigma^2 = \sum_{i=1}^k \sigma_i^2 \quad (1)$$

where σ^2 is total variance of mass of short longitudinal sections, and σ_i^2 is variance of mass of i-th component.

Given that the CV has a meaning of variation coefficient, we can write (2):

$$\sigma^2 = CV^2 \cdot T^2 \quad (2)$$

Substituting (2) into (1) we obtain (3):

$$CV_{limS}^2 \cdot T^2 = CV_{lim1}^2 \cdot T_1^2 + CV_{lim2}^2 \cdot T_2^2 + \dots + CV_{limk}^2 \cdot T_k^2 \quad (3)$$

After adjusting [9]:

$$CV_{lims} = \frac{\sqrt{\sum_{i=1}^k (CV_{limi} \cdot T_i)^2}}{T} \quad (4)$$

where CV_{lims} is quadratic limiting mass irregularity of blended yarn [%], CV_{limi} is quadratic limiting mass irregularity of component [%] defined as [10]:

$$CV_{limi} = \frac{100}{\sqrt{n_i}} \cdot \sqrt{1 + \left[\frac{v_{pi}}{100} \right]^2} \quad (4a)$$

where T is mean yarn count [tex], v_{pi} is variation coefficient of cross-section of fibre of i -th component [%], T_i is mean fineness of i -th proportion of components in the yarn [tex], determined as:

$$T_i = \frac{T \cdot p_i}{100} \quad (4b)$$

k is number of component, p_i is component representation in product (blending ratio) [%], n_i is mean number of fibres in the cross-section of i -th component, calculated as:

$$n_i = \frac{T \cdot p_i}{100 \cdot T_{vi}} \quad (4c)$$

and T_{vi} is mean fineness of fibres of given component [tex].

In many research works, e.g. [10-12], it is presented that the limiting mass unevenness of longitudinal fibre formation made from a one raw material is not directly affected by

the length of the fibres. As it can be seen from the equation (4a), the mean number of fibres in the cross-section of the product, i.e. the ratio of the fineness of the product to the fineness of fibres, has the main effect. These quantities also influence the limiting unevenness of blended product - see the equation (4). However, according to [13], the fibre length with the fibre fineness are important factor affecting the mass irregularity of yarn and hence the variability of its strength. Unequal fibre length of two components causes, according to [14], poor mixing of the fibres. Short fibres form clumps in the mixture. They do not open and create higher unevenness of yarn. Using the unequal fibre fineness, similar undesirable effect is achieved [14].

3 EXPERIMENT, RESULTS AND DISCUSSION

Combed yarns of nominal count 25 tex composed of 100% CO, 100% PL and various blending ratio of CO/PL were used for the experiment. Nominal fineness and length of CO fibres was: 1.65 dtex/ 29 mm, nominal fineness and length of PL fibres was: 1.6 dtex/ 38 mm. All yarns were produced from roving of nominal fineness 580 tex. Basic selected parameters of yarns with their 95 % confidence intervals are mentioned in the Table 1.

Table 1 Basic parameters of tested yarns

Blending ratio CO/PL [%]	Yarn twist [tpm]		Yarn count [tex]	
	Average value	95% conf. int.	Average value	95% conf. int.
100/0	738	(734 ; 742)	24.22	(24.13 ; 24.32)
87.5/12.5	736	(730 ; 742)	25.40	(25.07 ; 25.73)
75/25	739	(734 ; 744)	24.94	(24.85 ; 25.04)
62.5/37.5	735	(728 ; 742)	24.63	(24.41 ; 24.85)
50/50	704	(699 ; 709)	24.91	(24.81 ; 25.01)
37.5/62.5	718	(713 ; 723)	25.29	(24.40 ; 26.19)
25/75	701	(696 ; 706)	24.38	(24.01 ; 24.75)
12.5/87.5	702	(695 ; 709)	25.54	(25.23 ; 25.85)
0/100	692	(686 ; 698)	25.57	(25.29 ; 25.87)

The twist level for yarns with the cotton content more than 50% is higher than the twist level for yarns with higher proportion of PL. It is due to shorter cotton fibre length compared to PL staple fibres and also due to higher inter-fibre cohesion of PL fibres. Using fibres of greater length at the same count of the resulting yarn, lower intensity of twisting can be applied.

The yarn irregularity was measured simultaneously on the apparatus Uster-Tester IV-SX (obtained CV values are marked CV_{mass}) and on the device QQM-3 (CV values marked CV_{opt}). The sensor of the device QQM-3 was placed before the sensor of Uster Tester. Thus the measurement of the same length sections of yarn was ensured. Ten cops of yarns were tested from each blending ratio. Because of the memory capacity of the device QQM-3, these test conditions were set on both devices: yarn speed: 200 m/min, measurement time: 1 minute. The yarn irregularity was observed on these cut lengths: Uster Tester IV-SX: 1 cm, 1 m, 3 m, 10 m; QQM-3: 2 mm, 1 cm, 1 m, 3 m, 10 m. Examples of the results are shown in the Figures 2 and 3. In the Figure 2, the 5% percentile of CV_{mass} from the USTER®STATISTICS 2007 are also plotted for yarns 100% CO and 37.5% CO/ 62.5% PL. Values for other blending ratios of used combed yarns are not available. It is evident that the tested yarn achieves 5% of the cumulative frequency in terms of the observed parameter.

Pair correlation coefficients $\rho(\xi_i, \xi_j) = R$, expressing the degree of linear stochastic relation between the percentage representation of cotton in the yarn and yarn unevenness, are shown in the Table 2.

Statistically significant correlation coefficients are highlighted in bold. Their significance was tested according to the equation (5) [15]. We tested the hypothesis $H_0: \rho = 0$ against the alternative hypothesis $H_A: \rho \neq 0$ at the significance level $\alpha = 0.05$.

$$t = \frac{R\sqrt{n-2}}{\sqrt{1-R^2}} \quad (5)$$

where t is test statistics. Assuming the validity of the hypothesis H_0 the variable t has the Student distribution with $(n-2)$ degrees of freedom.

Table 2 Correlation coefficient between percentage of cotton content in the yarn and yarn unevenness

	% CO in yarn	
	Correlation coefficient R [-]	
	Uster Tester IV-SX	QQM-3
CV(2 mm)	-	0.944
CV(1 cm)	0.729	0.893
CV(1 m)	0.371	-0.111
CV(3 m)	0.064	-0.151
CV(10 m)	0.474	-0.602

In the case of CV on very short cut lengths (2 mm, respectively 1 cm), the results shows the significant influence of blending ratio CO/PL on the yarn irregularity. Compared with CV values from the device QQM-3, lower correlation coefficient between percentage of cotton in the yarn and CV measured by the apparatus Uster Tester may be caused also by, among others, a marked periodical short-term unevenness of yarn of the blending ratio 62.5% CO / 37.5% PL. This irregularity occurs negatively both in the spectrogram of yarn (Figure 2) and by increasing CV values, whose average value, compared with the others, appears as deviating. The CV value of this blended yarn measured by the device QQM-3 does not deviate. In the case of larger cut lengths, neither mass nor volume yarn irregularity changes significantly with increasing ratio of cotton fibres in the yarn. The possible reason of this phenomenon will be explained below.

Slight increase of yarn irregularity with the growing ratio of cotton in the yarn on very short cut length (Figure 2) can be explained by comparing measured (effective) yarn unevenness with its limiting irregularity.

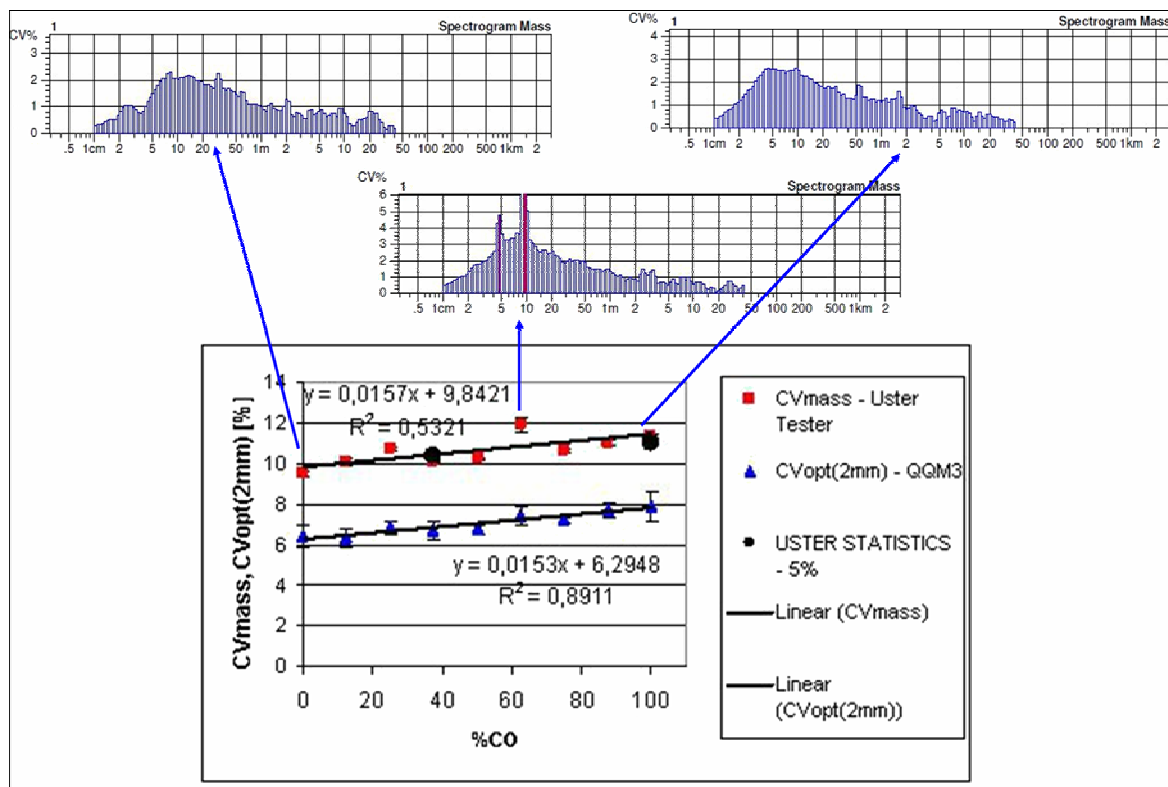


Figure 2 Influence of yarn irregularity CV_{mass} and $CV_{opt}(2\text{ mm})$ on cotton content [%] in yarn

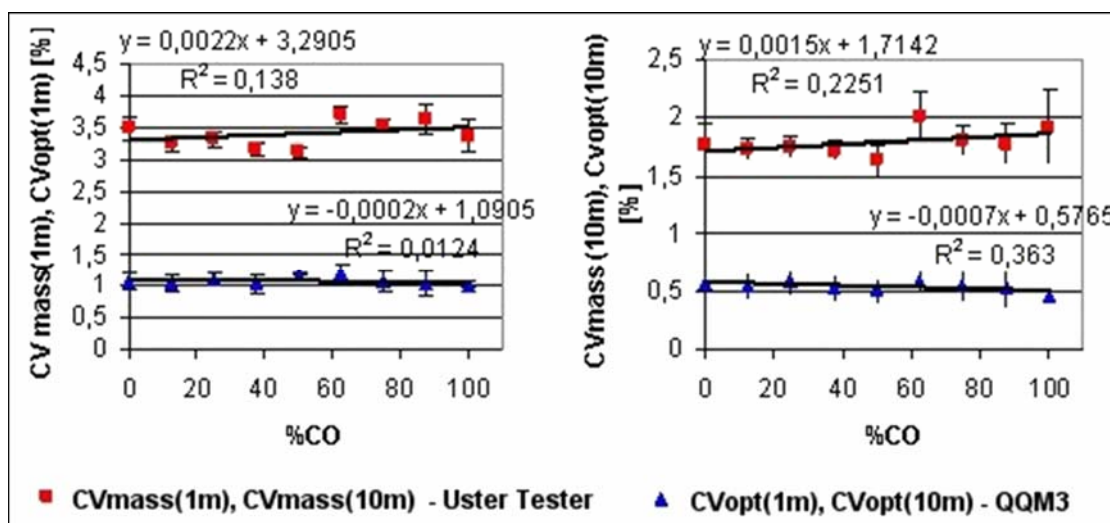


Figure 3 Influence of yarn irregularity $CV(1\text{ m})$ and $CV(10\text{ m})$ on cotton content [%] in yarn

3.1 Limiting and effective mass irregularity

The equation (4) was used to calculate the limiting mass irregularity of blended yarn. The influence of variation coefficient of fibre cross-section v_p was neglected considering to

practically the same small error for both used materials. For the calculation, the nominal yarn count $T = 25\text{ tex}$ as well as yarn count really measured T_{real} , mentioned in the Table 1, was used. The results are shown in the Table 3.

Table 3 Comparison of effective (measured) and limiting yarn mass irregularity

%CO	T_{real} [tex]	$CV_{mass_{eff}}$ [%]	$CV_{mass_{lim}}$ [%]			
			T_{real} $t_{CO} = 0.165$ tex $t_{PL} = 0.16$ tex	$T = 25$ tex $t_{CO} = 0.165$ tex $t_{PL} = 0.16$ tex	$T = 25$ tex $t_{CO} = 0.185$ tex $t_{PL} = 0.16$ tex	$T = 25$ tex $t_{CO} = 0.2$ tex $t_{PL} = 0.16$ tex
0	25.57	9.52	7.91	8.00	8.00	8.00
12.5	25.54	10.10	8.10	8.02	8.08	8.12
25	24.38	10.75	7.93	8.03	8.15	8.25
37.5	25.29	10.06	8.09	8.05	8.23	8.37
50	24.91	10.24	8.05	8.06	8.31	8.48
62.5	24.63	11.92	8.02	8.08	8.38	8.60
75	24.94	10.65	8.08	8.09	8.45	8.72
87.5	25.40	11.02	8.17	8.11	8.53	8.83
100	24.22	11.37	8.25	8.12	8.60	8.94

According to the theoretical knowledge, in addition to the quality of technological process, the mean number of fibres in the yarn cross-section, i.e. the ratio of mean fineness of longitudinal product and mean fineness of fibres, has the greatest influence on the yarn mass irregularity. The variability of fibre cross-section or fibre diameter has another influence on the mass irregularity, especially in the case of worsted yarns. The above mentioned factors of irregularity influenced by raw material are included in the theoretical formula for calculating limiting irregularity. We can see from the Table 3, fluctuations in yarn count ± 1 tex does not have any significant effect on the value of the limiting irregularity of tested blended yarn. In this case, the change of CV_{lim} is maximum 0.3%.

In the case of yarn of given count, mean number of fibres in the yarn (thus mean fineness of fibres of individual components), determines the level of limiting irregularity. If the fibre fineness of both components is equal, the change in the limiting unevenness of blended product in dependence on the blended ratio will be given only by the variability of the fibre cross-section of the component. In the case of CO/PL yarn, it will be an insignificant change (about 0.12% - see fifth column of the Table 3). In the blended fibrous product, the increase in the ratio of the component with higher value of linear density of fibre causes decreasing number of fibres in the cross-section. It will result in the

increase in limiting irregularity. This increase will be higher with the greater difference between fibre fineness of both raw materials, see the Table 3 and Figure 4.

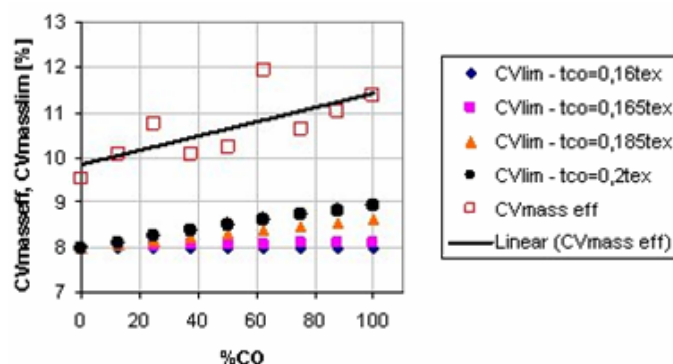


Figure 4 Effective and limiting mass irregularity in dependence on blending ratio of yarn ($T = 25$ tex, $t_{PL} = 0.16$ tex)

However, assuming nominal yarn count $T = 25$ tex and fineness of fibres $t_{CO} = 0.165$ tex and $t_{PL} = 0.16$ tex, it is evident, from the results, that yarn limiting irregularity does not increase significantly with a growing proportion of cotton. Even if the fineness of fibres was set incorrectly, the limiting mass irregularity ($CV_{mass_{lim}}$) would not grow so intensely as effective mass irregularity (CV_{mass}) increases. The reason is different length of used fibres and higher variability of cotton fibres in the comparison with PL fibres. Shorter cotton fibre length and its higher variability become important with the growing proportion of cotton in the yarn. It expresses

itself negatively in drafting mechanism where the CV of the resulting yarn increases due to increase in the number of floating fibres. Specifically, it is the increase in the so called induced systematic irregularity. It is an irregularity elicited from the latent irregularity by the draft and it occurs during yarn manufacturing [16]. Fibre length variability is not included at calculation of limiting mass irregularity, because the ideal technological process is assumed. The statistically significant increase in the yarn unevenness on very short cut lengths depending on the growing percentage ratio of cotton in the yarn compared with the statistically insignificant increase on the cut length of 1 m and larger can also be attributed to the combine effect of the fibre length, its variability and influence of drafting mechanism of the ring spinning machine. It contributes negatively to deepening unevenness on very short cut lengths. The influence of technological process on a change of mass irregularity of result product can be described by so called modulus of relative transfer function.

3.2 Modulus of relative transfer function

The modulus of relative transfer function is used for evaluation of balancing efficiency of dynamic system in term of mass irregularity. Each spinning machine with the continuous input and output of fibre formation is considered as the dynamic system [17, 18]. Knowledge of the modulus of relative transfer function also allows determining the structure of irregularity of the final product at parallel knowledge of the structure of irregularity of supply product.

Generally, the modulus of relative transfer function is a ratio of amplitudes of output and input signal relative to the corresponding mean values of fineness of output and input fibrous product.

$$|F^*(i\omega)| = \frac{\frac{A_1(\omega)}{T_{t1}}}{\frac{A_0(\omega)}{T_{t0}}} \quad (6)$$

where: $|F^*(i\omega)|$ is modulus of relative transfer function, $A_1(\omega)$, $A_0(\omega)$ is amplitude of output,

input signal, T_{t1} , T_{t0} is fineness of product in the machine output, input [tex] and ω is angular frequency of harmonic oscillation – harmonic component of output and input signal [s^{-1}].

The stationary random function expressing the course of the mass of short length sections of corresponding fibrous products in dependence on length of these products is considered as output (input) signal. Amplitudes of both signals are possible to be determined from corresponding spectrograms as amplitudes of harmonic components of courses of mass fluctuation on short sections with frequency ω . The angular frequency of signal oscillation ω can be replaced with wavelength λ according to equation (7), respectively (7a):

$$\lambda = \frac{2\pi}{\omega} v_2 \quad (7)$$

$$\lambda = \frac{2\pi}{\omega} v_1 \cdot P \quad (7a)$$

where: λ is wavelength [m], v_1 , v_2 is velocity of feeding, delivery rollers in the drafting arrangement [$m \cdot s^{-1}$] and P is draft ratio.

It is generally valid: if we get values of the modulus of relative transfer function $|F^*(\lambda)| > 1$, drawing system, as the dynamic system, does not balance the irregularity but increases it. The modulus value $|F^*(\lambda)| < 0.9$ means, according to [18], that corresponding system balances irregularity.

The theoretical modulus of relative transfer function of ideal drafting mechanism was derived in the work [19].

$$|F^*[\lambda]| = \left| P \cdot \frac{\sin \pi \frac{l}{\lambda}}{\sin \pi \frac{l}{\lambda} P} \right| \quad (8)$$

where $|F^*(\lambda)|$ is modulus of relative transfer function of drafting system as a function of λ ; P is draft ratio, l is fibre length [m] and λ is wavelength of harmonic component of mass irregularity [m].

As we can see from the equation (8), the modulus of relative transfer function is influenced by fibre length and draft ratio, which plays an important role. The modulus of relative transfer function of tested yarn composed of 100% CO is mentioned in the Figure 5. Due to the yarn nominal count (25 tex) and the roving nominal fineness (580 tex) it is considered draft ratio $P = 23$. Fibre mean length of 29 mm was used.

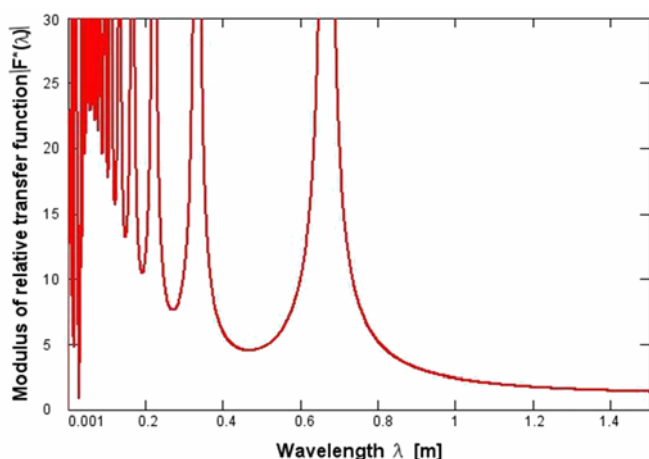


Figure 5 Modulus of relative transfer function of drafting system

From the course of modulus of relative transfer function (Figure 5) it is evident that drafting mechanism deepens irregularity on very short lengths. With increasing wavelengths, the modulus values decrease, thus the negative effect of drafting mechanism weakens.

The influence of fibre length on modulus of relative transfer function is mentioned in the Figures 6 and 6a. The draft ratio $P = 23$ and fibre length 29 mm, 33,5 mm and 38 mm was used for the construction of this curve. The range of chosen fibre length corresponds to the fibre length employed in the tested yarn. In the Figure 7a, the envelope curve of the modulus of relative transfer function is presented.

From the Figure 6a it is evident that modulus of relative transfer function, which corresponds to ideal draft, has slightly lower values with shortening fibre length at constant draft ratio. The draft ratio has much more important influence on the modulus of relative transfer function (Figures 7 and 7a). The greater the draft ratio, the modulus of relative transfer function has higher values on the same wavelength, i.e. the harmonic components of mass irregularity of resulting yarn are deepened.

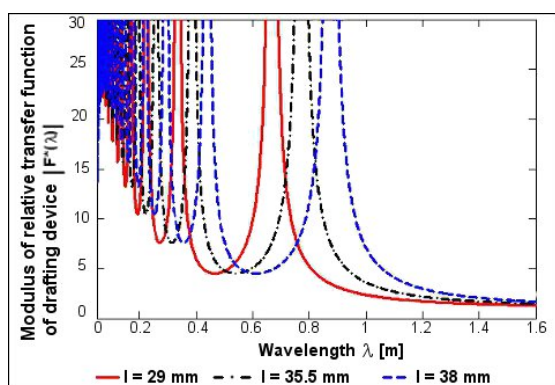


Figure 6 The courses of modulus of relative transfer functions of drafting system $|F^*(\lambda)|$ for various fibre length and constant draft ratio $P = 23$

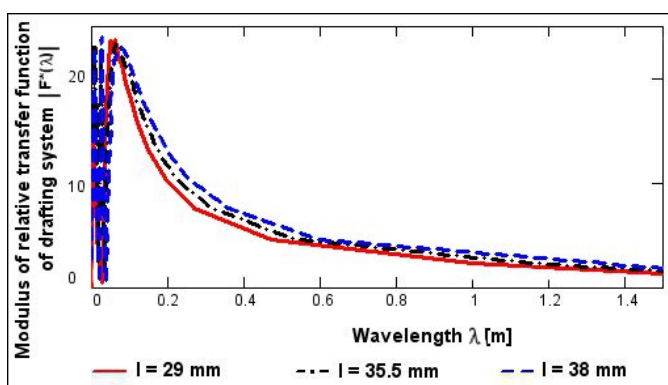


Figure 6a Envelope curves of modulus of relative transfer function of drafting system for various fibre length and constant draft ratio $P = 23$

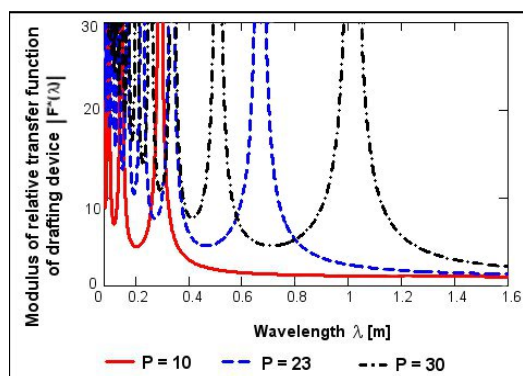


Figure 7 The courses of modulus of relative transfer functions of drafting system $|F^*(\lambda)|$ for various draft ratio and constant fibre length of 29 mm

Neither the draft ratio nor fibre length and its variability have important effect on the irregularity of yarn of different blend ratio from the length of 1 m. The modulus of relative transfer function was compiled for an ideal draft, which assumes that fibrous bundle of the same fibre length is drawn. With the growing variability of fibre length, which gains importance in the case of blended yarn with a higher proportion of cotton, the values of modulus of relative transfer function will be higher and thus short-term irregularity will be deepen. In the case of blended yarn, main influence will have component with higher variability of fibre cross-section (v_p [%]). The quadratic irregularity of the yarn will increase with growing proportion of this component in blended yarn. The results of the experiment also confirmed the relation between mass irregularity measured by the apparatus Uster Tester IV-SX and volume unevenness, determined optically using the device QQM-3, on very short lengths. As seen from the Figures 2 and 3, results from the device

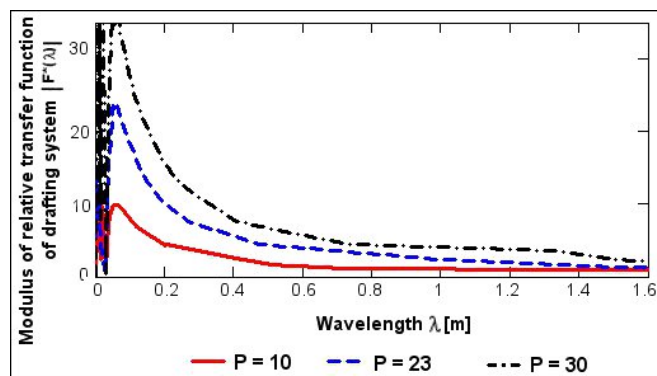


Figure 7a Envelope curves of modulus of relative transfer function of drafting system for various draft ratio and constant fibre length of 29 mm

QQM-3 achieved lower values. The correlation coefficients between appropriate CV are mentioned in the Table 4. Statistically significant coefficients are highlighted in bold. It is obvious that in the case of greater lengths the correlation coefficients between the two types of unevenness are statistically insignificant. The reason can be a different method of data treatment on individual devices when calculating the CV on longer cut lengths, such as another data filtering method [20], but also different formation of mass unevenness on longer cut lengths based on the irregularity created in the previous technological stages in the spinning mill. However, it should be noted that the relation between the mass unevenness measured by the apparatus Uster-Tester and volume unevenness obtained using QQM-3 device is valid always for the same type of yarn. Comparing the mass and volume unevenness across the range of types and fineness of yarn, the correlation is not valid [21].

Table 4 Correlation coefficient between volume (CV_{opt}) and mass (CV_{mass}) irregularity of combed yarn (fineness 25 tex)

		Correlation coefficient R [-]			
		Uster Tester IV-SX			
		CV_{mass} (1 cm)	CV_{mass} (1 m)	CV_{mass} (3 m)	CV_{mass} (10 m)
QQM-3	CV_{opt} (2 mm)	0.821	0.547	0.211	0.632
	CV_{opt} (1 cm)	0.791	0.615	0.260	0.592
	CV_{opt} (1 m)	0.357	0.566	0.408	0.278
	CV_{opt} (3 m)	0.075	0.567	0.563	0.178
	CV_{opt} (10 m)	-0.132	0.335	0.434	0.023

4 CONCLUSION

In this paper, the influence of the CO/PL blending ratio of combed yarn on mass and volume yarn irregularity was studied. Yarn mass irregularity was measured both by the capacitive principle using the apparatus Uster Tester IV-SX and optical method by the device QQM-3. The results were compared with the limiting mass unevenness. It was analyzed that both mass and volume irregularity is influenced especially with number of fibres in the yarn cross-section and variability of fibres cross-section together with negative influence of drafting mechanism. Fibre length and mainly its variability and occurrence of short fibres cause the increase in floating fibre bundles (i.e. fibres not controlled by drafting device). It results in increasing yarn mass irregularity. With the growing ratio of component, which has higher variability of fibre length, the yarn shows slight but statistically significant increase in the mass irregularity on short cut lengths due to the negative effect of drafting mechanism. It is also results in thickness, respectively attenuation of yarn cross-section, i.e. as fluctuation in the yarn volume. It is detected as a variation in the yarn diameter (i.e. volume variability) by the optical sensor of device QQM-3. Results of yarn irregularity expressed as CV measured both by the apparatus Uster Tester IV-SX and the device QQM-3 show the same trend in the case of short-term irregularity, the results from the device QQM-3 are lower. In the case of higher cut length, the correlation coefficient between mass and volume irregularity are statistically insignificant. The reason can be both different method of data processing of individual devices during calculating CV on longer cut lengths and different basis of formation of long-term mass irregularity compared to the formation of short-term irregularity, where the important cause is a direct effect of drafting mechanism.

5 REFERENCES

1. <http://www.usti.cz/vubas/qqm/> Accessed: 2010-09-13

2. <http://www.zweigle.com> Accessed 2007-10-30
3. <http://keisokki.com/> Accessed: 2010-09-13
4. <http://www.lawsonhemphill.com> Accessed: 2010-08-25
5. Slater K.: Yarn Evenness, Textile Progress Vol. 14(3/4), The Textile Institute, Manchester, 1986
6. Zellweger Uster: Zusammenhänge zwischen den Ergebnissen der Gleichmässigkeitsprüfung und den Aussehen der fertigen Gewebe und Gewirke. Uster News Bulletin, No. 15, pp. 3 – 36, 1971
7. Zellweger Uster: Neue Möglichkeiten der Analyse von Masseschwankungen an Garnen, Vorgarnen und Bändern, Uster News Bulletin, No. 35, pp. 6 - 18, 1988
8. [<http://www.uster.com> Accessed: 2012-09-13
9. Uster Technologies AG: Uster Tester IV Application Handbook, V1.0/400 106-04010, Uster, 2001
10. Martindale J.G.: Journal of the Textile Institute 36, T35, 1945
11. Neckář B., Ibrahim S.: Structural Theory of fibres assemblies and yarns, part I – Structure of fibrous assemblies, Technical University of Liberec, Liberec 2003
12. Ginsburg L.N., et al: Dynamika osnovnich procesov prjadenija I, formirovanie i vyvornivanie voloknistogo potoka, Izdatelstvo lëgkaja industrija, Moskva 1970
13. Lawrence C. A.: Fundamentals of spun yarn technologies, CRC Press, New York, ISBN 1-56676-821-7, 2003
14. Vaverka J.; Machuta K., Rybníkář J.: Teorie a praxe předení ve vlnářském průmyslu - česaná příze, SNTL Praha, Praha, ISBN 80-03-00133-1, 1990
15. Meloun M.; Militký J.: Statistické zpracování experimentálních dat, PULS, Praha, ISBN 80-85297-56-6, 1994
16. Ursíny P.: Mass irregularity changes in spinning technology, Fibres and Textiles Vol.10 (2), pp. 62-65, ISSN 13350617
17. Balda M.; Bošek M.; Dráp Z.: Základy automatizace, SNTL, Praha, 1968
18. Rohlena V., et al: Bezvřetenové předení, SNTL Praha, 1974
19. Sevost'yanov A.G., et all.: Kinematičeskaja teorija vytjagivanja voloknistovo produkta. Izvestija vyššich učebnych zavedenij, Technologija textilnoj promyšlenosti, Vol. 5, pp. 68-75, 1967
20. Militký, J., Ibrahim S., Křemenáková D., Mishra R., Moučková E., Mvubu M.B.: Comparative study of yarn diameter measurements, 16th International Conference STRUTEX Structure and Structural Mechanics of Textile Fabrics, CD-rom edition; ISBN 978-80-7372-542-6, December 2009, Technical University of Liberec, Liberec, 2009
21. Mvubu M.B.: Characterization of Yarn Diameter Measured by Different Systems, Diploma work, Technical University of Liberec, Liberec, 2010

ANALÝZA NESTEJNOMĚRNOSTI SMĚSOVÝCH BAVLNÁŘSKÝCH PŘÍZÍ

Translation of the article
Analysis of cotton blended yarns irregularity

Příspěvek se zabývá analýzou nestejnoměrnosti bavlnářských přízí různých směsových poměrů CO/PL. Je hodnocena úroveň nestejnoměrnosti (CV) vzhledem k procentuálnímu zastoupení bavlny v přízi. Nestejnoměrnost přízí je měřena kapacitním (Uster Tester IV-SX) a současně optickým způsobem (QQM-3). Z výsledků vyplynul statisticky významný vliv procentuálního zastoupení bavlny na CV příze na velmi krátkých úsečkách. Pro objasnění získaných výsledků hmotové nestejnoměrnosti je proveden rozbor limitní nestejnoměrnosti příze ve vztahu k parametrům použité suroviny a jemnosti příze, současně je aplikován modul poměrné přenosové funkce průtahového ústrojí. Jsou porovnávány výsledky měření hmotové a objemové nestejnoměrnosti.

DESCRIPTION OF BINDING WAVES USING THE FOURIER SERIES

B. Kolčavová Sirková

*Technical University of Liberec, Faculty of Textile Engineering, Department of Textile Technologies, Liberec,
Studentská 2, 461 17 Liberec 1, Czech Republic
telephone: +420 48 535 3274; Fax: +420 48 535 3542
e-mail: brigita.kolcavova@tul.cz*

Abstract: *Many attempts have been done in the past to find a suitable model describing the binding cell, i.e. to express mathematically the shape of the binding wave in a given thread crossing in the fabric in the steady state. Peirce model, Ollofsson model, hyperbolic model, parabolic shapes are known as the most used models. These models are related to the plain weave. Other than plain kinds of interlacing could theoretically rise from models created before. However, additional mathematical formulations used for expressing the un-regularity of interlacing in bindings, that are more complex, describe the real binding conditions in a not very satisfying manner. This paper is focused on introduction of mathematical model for description of binding waves in plain as well as non-plain threads interlacing in woven fabric using the Fourier series.*

Key words: *Woven fabric, Weave, Model, Structure, Interlacing.*

1 INTRODUCTION

The fabric as a plain product is created by mutual interlacing of two sets of threads. The manner of the mutual interlacing of threads defines the final structure of fabric. The shape of the binding wave and basic geometry of the binding cell changes according to the dimension and number of threads in the weave repeat or in the binding cell. The geometry of the binding point in the plain weave for the mathematical model used later is based on the Brierley theory of the tight weave. The geometry of the binding cell for other than plain weaves was derived from plain weave. Looser interlacing of the fabric depends on the type of used material and on the type of machine. Interlacing and own shape of the binding wave in the longitudinal section and in the transverse section is identical for plain weave and for every basic weave. It is only the detailed parameters which determine the final structure and properties of the fabric. Geometry of the binding cell is possible to describe on the basis of under-mentioned parameters:

1. Dimensions are given by the distances of both systems of threads,
2. The interlacing of warp and weft is defined by the heights of binding waves,
3. Basic parameters of both systems of threads: yarn count, setting of threads, yarn diameters.

2 MATHEMATICAL MODEL FOR DESCRIPTION OF BINDING WAVE USING THE FOURIER SERIES

The description of the shape of binding waves can be provided in the fabric in the longitudinal cross-section (the shape of the binding wave of the warp thread) and in the transverse cross-section (the shape of the binding wave of the weft thread) in order to define the mutual position of the warp threads towards weft threads.

Due to spatial threads distribution in the cross section of a cloth the shape of the binding wave obtains the form which is near to the harmonic sinus course. That leads to the idea to approximate the binding wave by a sum of Fourier series. For the fabric weave it is characteristic that the pattern of binding is

repeated regularly (periodically) across the whole fabric width, and that it is continuous, see Figures 1, 2.

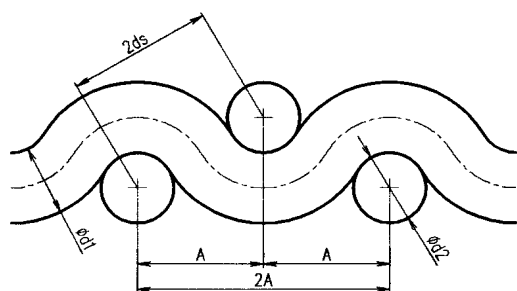


Figure 1 Geometry of the plain weave

The Fourier approximation respects this periodicity and shape of the binding wave, in the contrary to the above-mentioned models of single threads crossings. In our case of the periodically repeated pattern of thread waves, it means to substitute the binding wave by a system of sine curves with increasing frequencies (decreasing wavelengths), with different amplitudes and phase shifts. Apart from the approximated course, we obtain by approximations using the sum of Fourier series also the s.e. spectral characteristic of

the course. Spectral characteristic consists of amplitude and phase characteristics of individual wavelengths. The wavelengths are the whole fractions of the basic wavelengths of the pattern on the interval of the binding repeat (0, binding repeat).

The shape of the binding wave or its course can be possibly obtained reversibly from the spectral characteristics by two methods:

1. Approximation of the whole wave course by a partial sum of Fourier series (harmonic synthesis). The series is given by the table of equidistant co-ordinates which will be obtained from the real fabric (real longitudinal and transverse sections) by the image analysis (using the software NIC-ELEMENTS).
2. There is a tendency to avoid laboured and tardy procedure of the creation of the cross sections. The values of the course of one binding wave will be obtained by substitution of the wave shape by a well-known analytic function $f(x)$, or created by a sum of functions defined on the specified interval T . The interval is given by the width of the repeat of binding.

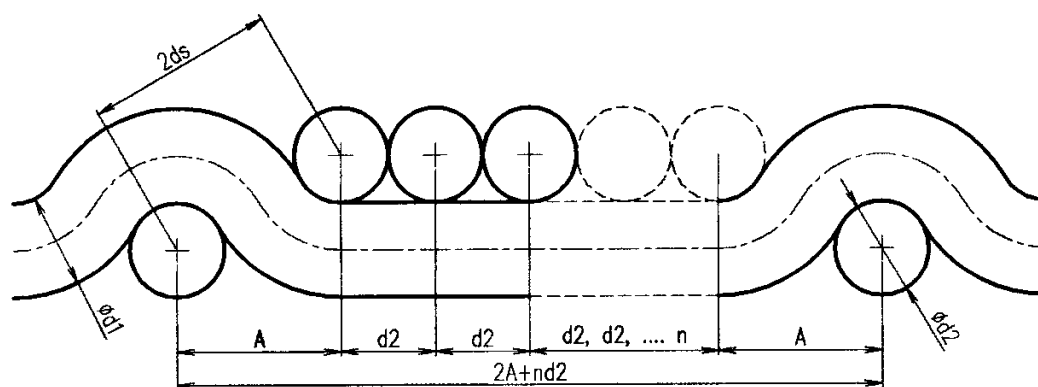


Figure 2 Geometry of the higher derived bindings

where: A [mm] – threads distance, d_1 , d_2 , d_s [mm] – yarn diameter - warp, weft, mean

The approximation is given by the expansion of the function "f (x)" in Fourier series in the form (1):

$$\frac{a_0}{2} + \sum_{n=1}^{\infty} (a_n \cos(nx\omega) + b_n \sin(nx\omega)) \quad (1)$$

where: a_0, a_n, b_n ...the coefficients of series.

Considering, that function f (x) is a periodical function with period 2π and f (x), f'(x) are piecewise continuous in the interval $(-\pi, \pi)$, coefficients of Fourier series are given by eq. (2), (3):

$$a_n = \frac{1}{\pi} \int_{-\pi}^{\pi} f(x) \cos(nx) dx \quad (n=0, 1, 2, \dots) \quad (2)$$

$$b_n = \frac{1}{\pi} \int_{-\pi}^{\pi} f(x) \sin(nx) dx \quad (n=1, 2, 3, \dots) \quad (3)$$

In every point x, where f (x) is continuous, it holds (4):

$$\frac{a_0}{2} + \sum_{n=1}^{\infty} (a_n \cos(nx) + b_n \sin(nx)) = f(x) \quad (4)$$

Moreover, in every point x, where f (x) is discontinuous, it holds (5)

$$\begin{aligned} \frac{a_0}{2} + \sum_{n=1}^{\infty} (a_n \cos(nx) + b_n \sin(nx)) = \\ = \frac{1}{2} [f(x+0) + f(x-0)] \end{aligned} \quad (5)$$

Herewith f (x+0), f (x-0) are limits on the right, limits on the left of the function f (x) in the point x. For periodical function f (x) with period R and with basic interval (0, R), the relation is valid analogous as in the antecedent case:

$$\frac{a_0}{2} + \sum_{n=1}^{\infty} [a_n \cos(\frac{nx2\pi}{T}) + b_n \sin(\frac{nx2\pi}{T})] = f(x) \quad (6)$$

$$= \frac{1}{2} [f(x+0) + f(x-0)] \quad (7)$$

where:

$$a_n = \frac{1}{T} \int_0^T f(x) \cos(\frac{nx2\pi}{T}) dx \quad (n=0, 1, 2, \dots) \quad (8)$$

$$b_n = \frac{1}{T} \int_0^T f(x) \sin(\frac{nx2\pi}{T}) dx \quad (n=1, 2, 3, \dots) \quad (9)$$

In the case that:

- the function f (x) is an odd function (i.e. it is $f(-x)=-f(x)$), then according to calculation of the coefficients of Fourier series it holds: $a_n=0$ for $n=0, 1, 2, \dots$ the series contains only sine members.
- the function f (x) is an even function (i.e. it is $f(-x)=f(x)$), then according to calculation it holds: $b_n=0$ for $n=1, 2, \dots$ the series contains only constant member $a_0/2$ and cosine members.

The function f (x) as theoretical shape of binding wave can be substituted by the well-known analytical discontinuous function. The function is defined on the specified interval R that is number of the binding repeat. Four theoretical idealised shapes of interlacing were chosen under mentioned shapes:

1. linear description of the central line of the binding wave,
2. circular arch description of the central line of the binding wave,
3. parabolic description of the central line of the binding wave,
4. hyperbolic description of the central line of the binding wave.

Linear variants only in the papers will be introduced.

3 STUDY OF THE APPROXIMATIONS OF BINDING WAVE ON THE BASIS OF LINEAR DESCRIPTION OF CENTRAL LINE USING THE FOURIER SERIES

The expression of the area and the spatial geometry is important not only for description of the final fabric structure but also for description of the specific weaving process. The shape of linear description of central line in the interlacing as we can see doesn't correspond with real shape of binding wave, see Figure 3.

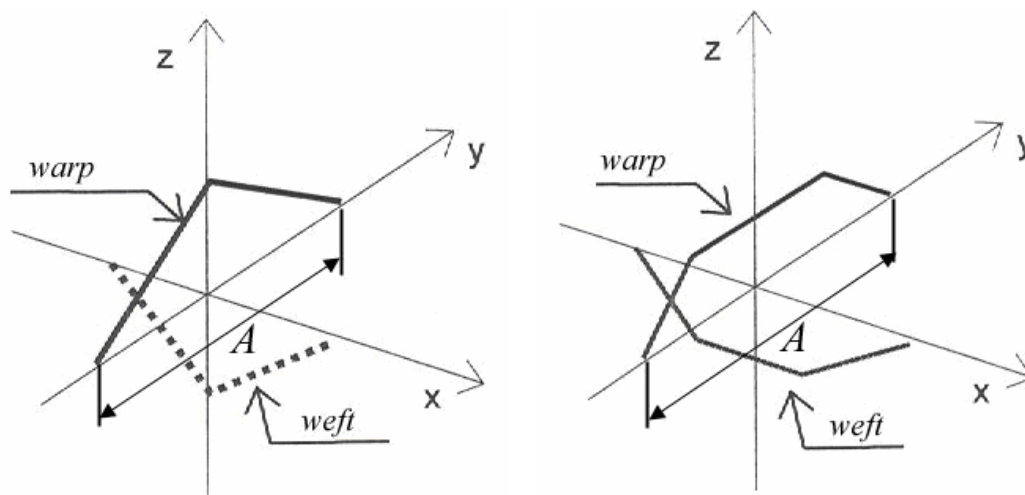


Figure 3 Linear description of central line of plain and non-plain interlacing

Coefficient of Fourier series are given by eq. (10), (11)

$$a_n = \frac{1}{T} \left[\int_0^{T/2} \left(\operatorname{arctg} \frac{2H1}{T} x - H1 \right) \cos\left(\frac{nx2\pi}{T}\right) dx + \int_{T/2}^T \operatorname{arctg} \frac{2H1}{T} \left(x - \frac{T}{2}\right) + H1 \cos\left(\frac{nx2\pi}{T}\right) dx \right] \quad (10)$$

$$b_n = \frac{1}{T} \left[\int_0^{T/2} \left(\operatorname{arctg} \frac{2H1}{T} x - H1 \right) \sin\left(\frac{nx2\pi}{T}\right) dx + \int_{T/2}^T \operatorname{arctg} \frac{2H1}{T} \left(x - \frac{T}{2}\right) + H1 \sin\left(\frac{nx2\pi}{T}\right) dx \right] \quad (11)$$

where: T – repeat of weave, $H1$ – height of binding wave.

The float part is substituted by abscissa for other than plain weave (non-plain interlacing). This description is applicable in every interlacing of basic bindings as well as of higher derived bindings.

In this case, linear description of central line is important as input function for theoretical mathematical modelling and simulation of threads interlacing in woven fabric. From mathematic modelling of woven fabric geometry based on Fourier series we obtain approximated course of threads interlacing as well as spectral characteristic of the interlacing.

The waviness e_{warp} , e_{weft} , of interlacing is given by the height of binding wave in the woven fabric. The height of the warp binding wave h_{warp} and the height of the weft binding wave h_{weft} , is the maximum displacement of thread axis normal to plane of woven fabric. The height of interlacing wave for individual threads is given by eq. (12, 13)

$$h_{\text{warp}} = e_{\text{warp}} \cdot d_s \quad (12)$$

$$h_{\text{weft}} = (1 - e_{\text{warp}}) d_s \quad (13)$$

$$d_s = \frac{d_{\text{warp}} + d_{\text{weft}}}{2} \quad (14)$$

where: h_{warp} , h_{weft} [mm] – height of binding wave (warp, weft), e_{warp} , e_{weft} [] – waviness of warp and weft threads, d_s [mm] – mean diameter of threads.

On the basis of theoretical description based on Fourier series the height of binding wave is given by mathematical model as well as the sum of Fourier series. Maximal value of height of binding wave is possible to obtain using of first harmonic component for approximation of central line of interlacing, see Figures 4, 7 and 10. Other harmonic components optimize the shape of binding wave and the sum is possible to decrease the value of final height of binding wave in cross-section of woven fabric.

Plain weave – represents the basic interlacing of ends and picks. Only two different interlacing threads appear in the binding repeat in the longitudinal section or in

the transverse section. Result in the spectral characteristic of the binding plain repeat will be combined from two of the identical spectral characteristics of the binding waves (first and second binding waves in the binding repeat).

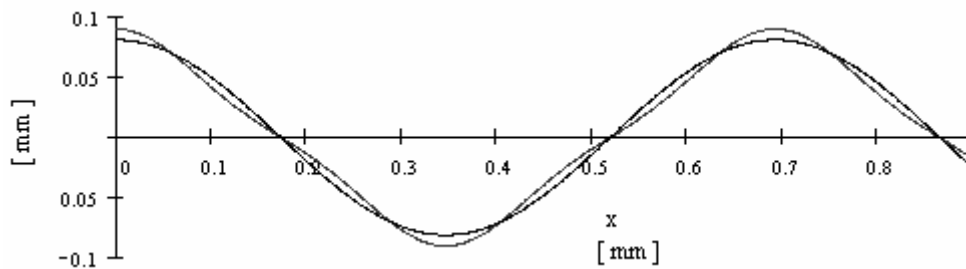


Figure 4 The shape of the approximated binding wave in the plain weave

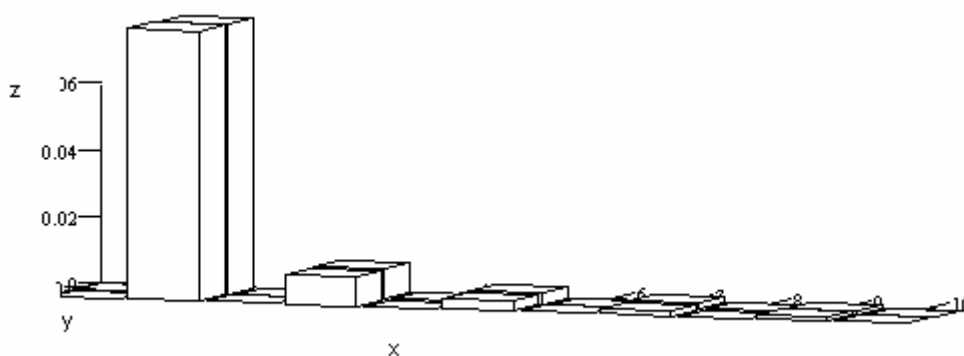


Figure 5 Spectral characteristic of the binding waves in longitudinal (transverse) section of plain weave, where: x – the binding waves of the binding repeat [], y – wavelengths of the harmonic components [mm], z – amplitudes of the harmonic components [mm]

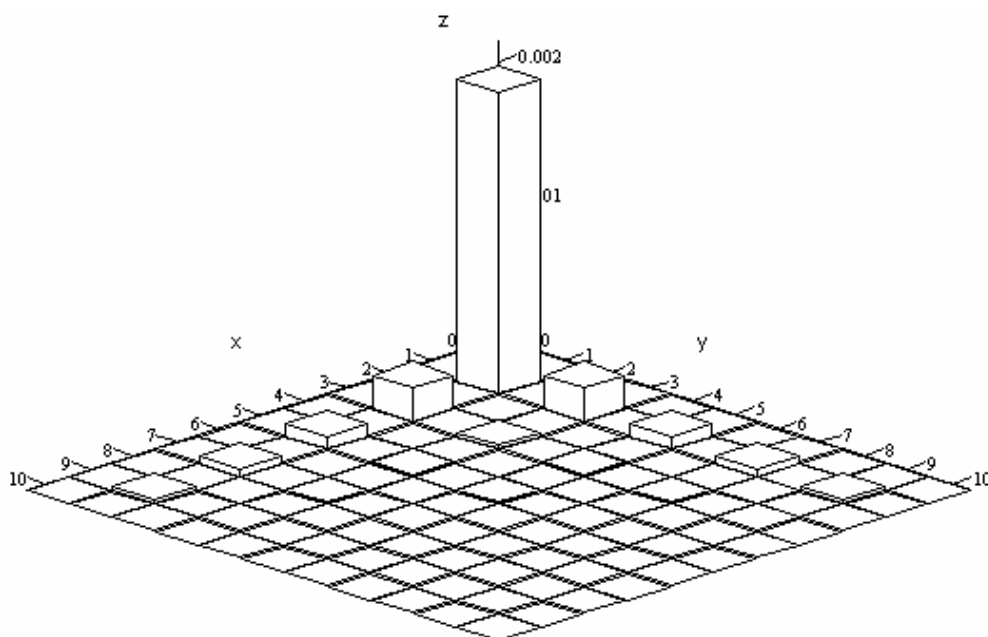


Figure 6 Spectral characteristic of plain weave, where: x – harmonic components of the transverse section, y – harmonic components of the longitudinal section, z – amplitudes of the harmonic components [mm]

Twill weave – in comparison with the plain weave has looser interlacing. In this twill weave can be reached higher setting. Individual binding waves in the binding repeat

are identical in the longitudinal and in the transverse section. It is valid for the basic twill weaves only.

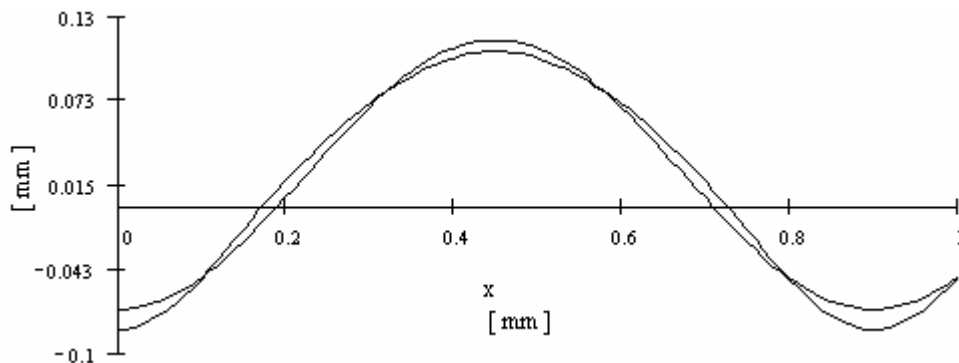


Figure 7 The shape of the approximated binding wave in the twill weave (repeat=4x4)

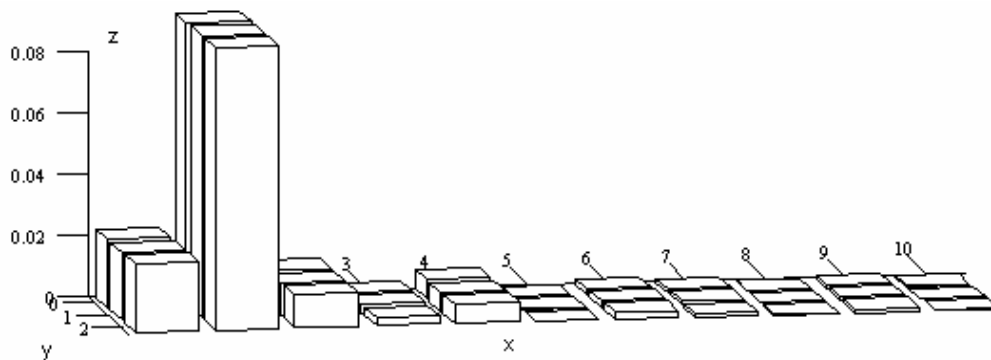


Figure 8 Spectral characteristic of the binding waves in longitudinal (transverse) section of twill weave, where: x – the binding waves of the binding repeat [], y – wavelengths of the harmonic components [mm], z – amplitudes of the harmonic components [mm]

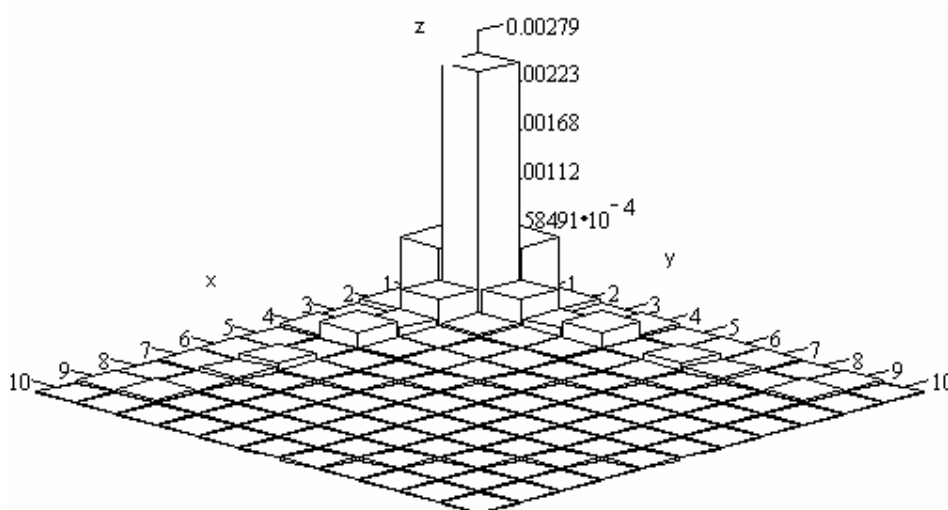


Figure 9 Spectral characteristic of twill weave (repeat=4x4), where: x – harmonic components of the transverse section, y – harmonic components of the longitudinal section, z – amplitudes of the harmonic components [mm]

Satin weave – in comparison with the plain and the twill weave satin weave has looser interlacing. At this weave higher setting can be reached. Individual binding waves in the

binding repeat are identical in the longitudinal and in the transverse section. It is valid for the basic satin weaves only.

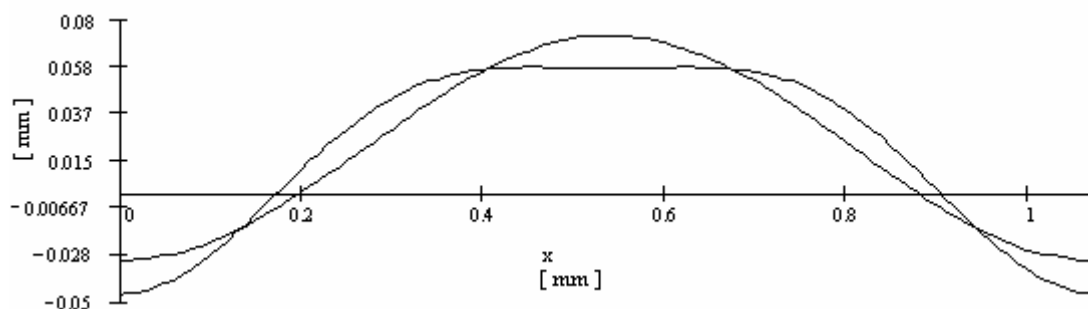


Figure 10 The shape of the approximated binding wave of the satin weave

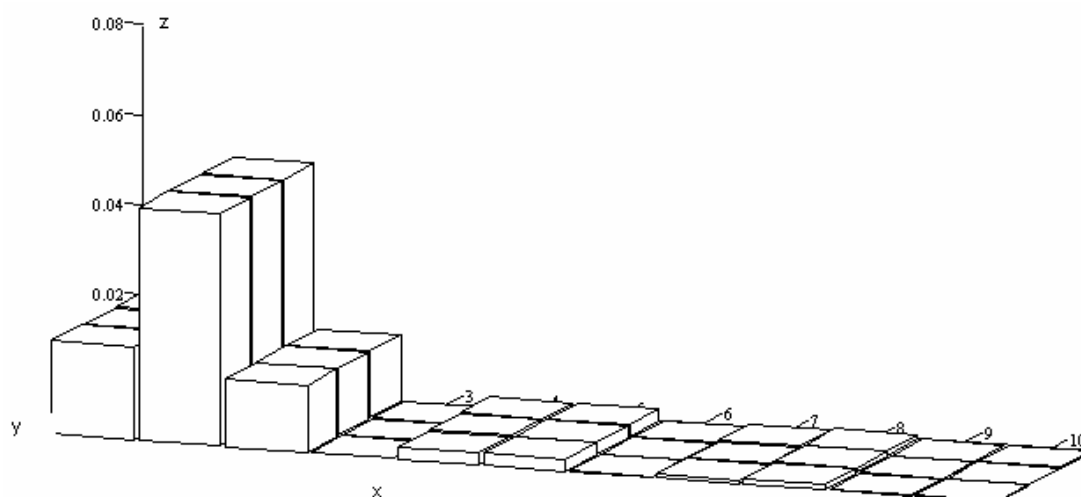


Figure 11 Spectral characteristic of the binding waves in longitudinal (transverse) section of satin weave, where: x – the binding waves of the binding repeat [], y – wavelengths of the harmonic components [mm], z – amplitudes of the harmonic components [mm]

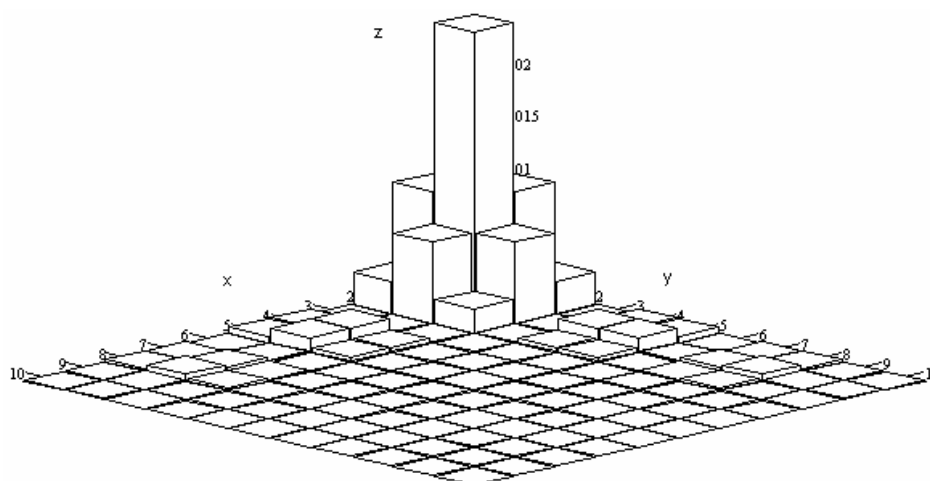


Figure 12 Spectral characteristic of the threads interlacing in satin weave, where: x – harmonic components of the transverse section, y – harmonic components of the longitudinal section, z – amplitudes of the harmonic components [mm]

4 CONCLUSION

All necessary information about the fabric can be deduced from the description of mutual relations of the binding cell. Basic at the every model is to describe the real interlacing, real binding wave in the fabrics. Above-mentioned models using a partial sum of Fourier series, we can use as possibly substitution of the classic models because description of the shapes of binding waves is continuous and smooth functions as in the real bidding wave. Except of the approximated course at the above-mentioned of the models arise spectral wavy spectrum, which we can use as the characteristics of the interlacing. Evaluation of the fabric by means of the Fourier spectral characteristics is possible separately for the longitudinal and transverse section as well as together in the both sections. It is impossible to achieve the whole spectral characteristic of the fabric. The spectral characteristics react on the basic changes in the fabric:

- the change of the flexural rigidity – this change leads on the change of the shape of the central binding line in the interlacing,
- the change of the thread's tension – this change leads to the change of the waviness and deformation of the binding wave,
- the change of the thread's position in the floating part, the change of the density – this change leads to the change of the thread's distance,
- the change of the weave.

Other exploitation of the spectral characteristic is possible for evaluation of the mechanical properties (anisotropy and isotropy of the fabric) in virtue of change of the symmetry on the asymmetry of the interlacing in consequence of change of the interlacing in longitudinal as well as in transverse sections.

The object of this the present work is to find the model for description of the binding waves and characteristic of the binding wave or characteristic of the repeat of binding (spectral characteristic), which will react on the deviation in the real interlacing.

5 REFERENCES

1. Nosek S.: Weaving theory I, Dům techniky, Pardubice 1988
2. Křemenáková D., Kolčavová Sirková B., Mertová I.: Internal standards, Research centre, Liberec 2004
3. Szosland J., 'Kształowanie własności tkanin poprzez kształtowanie fazy ich struktury' (in Polish, 'Designing of woven fabric features by designing the phase of their structure'), *Architektura Tekstyliów*, No. 1-3, 1999
4. Wang Y., Sun X.: Determining the geometry of textile performs using finite element analysis, 15th Annual Technical Conference for Composites, Sept., 23-27, 2000
5. Backer S.: The relationship between the structural geometry of textile and its physical properties, I: Literature review. *Text. Res. J.* 18, 650-658, 1948
6. Textile Protection And Comfort Center, North Carolina State University, <http://www.tx.ncsu.edu/tpacc/comfort-performance/kawabata-evaluation-system.cfm>
7. Kolčavová Sirková B.: The influence of threads interlacing on the mechanical properties of the woven fabrics, IMCEP 2003 Innovation and modelling of clothing engineering processes, University of Maribor, Maribor, Slovenia, 2003
8. Behera B.K., Hari P.K.: Woven textile structure, Theory and applications, Woodhead Publishing Limited, ISBN 978-1-84569-514-9 (book), 2010
9. Křemenáková D., Mertová I., Kolčavová Sirková B.: Computer aided textile design 'LibTex', *Indian Journal of Fiber & Textile Research*, India Vol.33, 40-404, December 2008
10. Milašius V.: Woven Fabric's Cross-Section: Problems, Theory, and Experimental Data, *Fibres and Textiles in EE* No 4(23), 48-50, 1998
11. Oloffson B.: „A general model of a fabric as a geometric mechanical structure” *J. Textiles Isnt.* 55(11), 541-557, 1964
12. Ozgen B., Gong H.: Yarn geometry in woven fabric, *Textile Research Journal* 81(7), 738-745, May 2011
13. Kemp, A. J.: *Textile Institute* 49, T44, 1958
14. Duckett K.E., Cheng C.C.: A Discussion of The Cross-point Theories, *Journal of the Textile Institute* 69(2 & 3), 55-59, February 1978
15. Keefe M.: Solid Modeling Applied to Fibrous Assemblies PartII: Woven Structure, *Journal of Textile Institut* 85(3), 350-358, 1994
16. Masajtis J.: Analiza strukturalna tkanin, Polska Akademia Nauk Oddział w Łodzi, Komisja Włokkiennictwa, Łódź 1999
17. Barburski M., Masajtis J.: Modelling of the Change in Structure of Woven Fabric under Mechanical Loading. *Fibres & Textiles in Eastern Europe* Vol. 17, No. 1(72), 39-44, , January/March 2009

POPIS VAZNÉ VLNY V PROVÁZÁNÍ S VYUŽITÍM SOUČTU FOURIEROVY ŘADY

Translation of the article
Description of binding waves using the Fourier series

Byla vytvořena celá řada pokusů nalézt vhodný model popisující vaznou buňku (vazný bod), tj. vyjádřit matematicky tvar vazné vlny v daném zakřížení nití ve tkanině v ustáleném stavu. Peirceův model, Olofssonův model, hyperbolický model, parabolický tvar, jak je známo jedná se o nejznámější modely, které se vztahují k plátnové vazbě. Popis jiného než plátnového provázání je možné odvodit od výše uvedených modelů. Obecně navrhované matematické výrazy popisující nepravidelnosti v provázání nití ve tkanině málo vystihují skutečné provázání. Článek je zaměřen na představení matematického modelu využívajícího součtu Fourierovy řady pro popis vazné vlny v plátnových a neplátnových vazbách ve tkanině.

THE DEVELOPMENT APPROACHES TO THE NEW FORMS OF CLOTHES CREATION WITH SIGNS AND SYMBOLS OF TRIPILL CULTURE BY DESIGNING METHODS

O.V. Kolosnichenko

*Faculty of Design, Kiev National University of Technologies and Design
Nemirovicha-Danchenka str. 2, 01011 Kiev, Ukraine
3212793@gmail.com*

Abstract: *The paper deals with modern methods of designing, the use of which allows to develop new forms of contemporary women clothes with the system of signs and symbols of Tripill culture. The use of the principles of new forms obtaining, based on the creative concept, makes it possible to receive a large number of new models in the system "clothes-human-being-environment". The ways of improvement of designing and new forms of contemporary women clothes have been determined.*

Key words: *Trippil culture, the creation of new forms of clothing, morphological matrix design and decorative elements.*

1 INTRODUCTION

The actuality of the topic of investigation is caused by the necessity of modern science in the new approach to the investigation of the peculiarities of modern fashion development. It is due to the great changes in modern trends; mutual penetration of cultures under global social informatization; the appearance of a number of signs and symbols (in costume, interior and life in general), their untraditional combination technologies.

It makes possible to create the new forms, ornamentation and materials in order to raise the articles design level and the production mobility. This will speed up the development of fashion trends. There are no publications on the problem of interrelation of symbols and colours in the form and material of Tripill costume nowadays. Informative signal costume system in relation to its colour visualization, and also the accordance of its sense to the situational environment has not been yet investigated. It is also known [1-4] that informative-signed system is in-between notion. On the one hand, symbol is an element, creating the meaning of the informative-signed system "costume" and has definite characteristics and functions. On the other hand, contemporary costume is

informative-signed system with symbol being an element. The power and importance of Tripill culture science is very important in clothes designing. It gains popularity nowadays due to the arising of national consciousness, the desire of the society to come back to its routes using the ancient traditions in modern life.

It should also be noted that methods of system approach are not fully applied to the investigation of Tripill costume that makes the development of new approach to the designing of modern forms of clothes for different purposes.

2 THE OBJECT, METHODS AND TASK OF INVESTIGATION

The object of investigation is the system of signs and symbols of Tripill culture. The analysis and systematization of sign system of Tripill culture allows to structurize the forms of Tripill statuette and to determine the anthropomorphic plastic women clothes. To form the creative concept the sign-communicative functions of costume, interconnection of symbol - source with costume, Tripill symbols on statuettes and clothes (Figure 1) [1] have been investigated; protective sign system, family relations have

been analysed and systemized (Figure 2) [2]. Tripill plastic according to the geometric forms of women image in the typology of Tripill statuettes (as to the time period) has been structurized; morphological matrix of designing-decorative elements of Tripill clothes, morphological matrix of designing-decorative elements of contemporary clothes using Tripill elements; schematic description of product modelling on the bases of Tripill culture has been performed.

The purpose of investigation is the development of new forms in the collection of the modern women clothes, the creation of contemporary women clothes with the use of sign and symbol system of Tripill culture on the basis of new tasks in clothes designing and new technological solutions. The methods of investigation are mainly based on empiric study and associated methods grounded on the creative concept. The analysis and synthesis of the modern designing methods being used during the

experimental elaboration of signs and symbols on the patterns of new forms of clothes have been used.

- the development of “costume-human-being-environment” system, the analysis and systematization of Tripill culture and clothes; determination of clear functional relations between the environment, its elements and processes being created with a human-being;
- the structural analysis of Tripill plastics by geometrical forms of woman depiction;
- the development of morphological matrix of designing-decorative elements of Tripill clothes;
- the construction of patterns of women clothes using signs and symbols of Tripill culture;
- making up the creative collection as to the principles of rolling up of received patterns into the samples of the new forms of clothes.

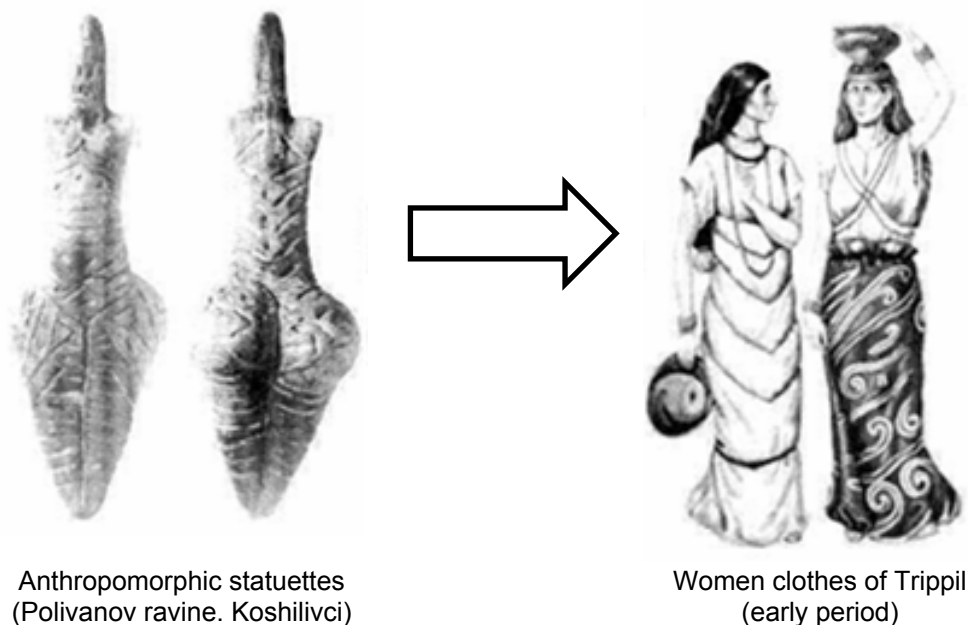


Figure 1 The connection of Tripill symbols on statuettes with those on clothes

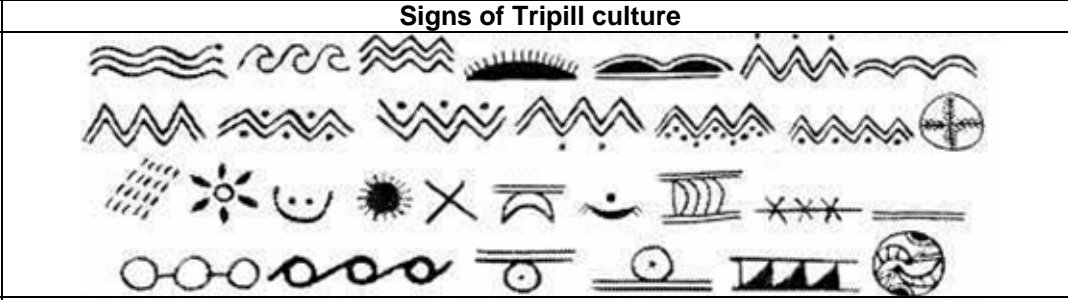

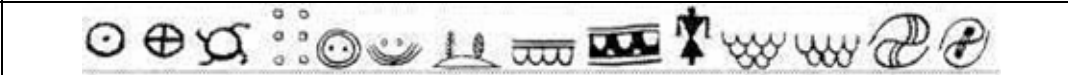
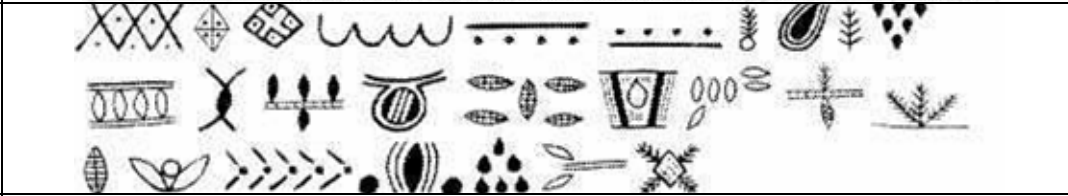
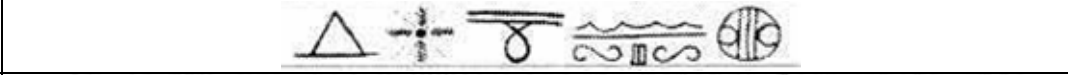
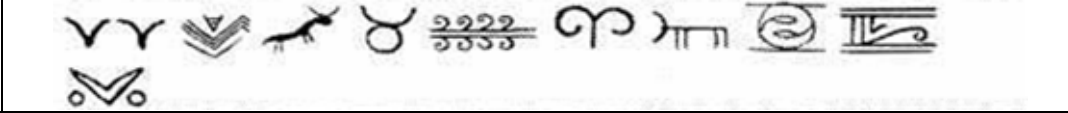
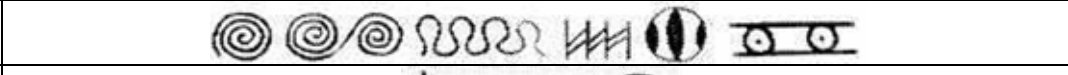
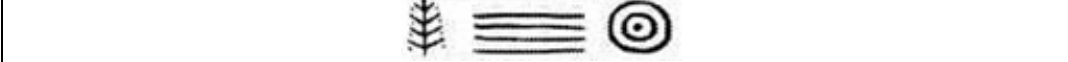


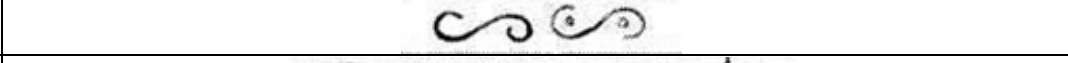


Group of signs	Signs of Tripill culture
Nature	
Ward	
Family	
Fertility	
Food	
Animals	
Time	
Life	
Victory	
The beginning and end	
Changes	
Wealth	
Unity	

Figure 2 Classification of Tripill culture signs

3 THE RESULTS AND DISCUSSION

Practical meaning of scientific investigation lies in the active mastering of modern scientific designing methods, formed on the fundamental and applied sciences meeting point, mathematics and art, and also in creating scientific ideas in order to develop modern technological solutions as to the products, characterized by novelty of artistic image, creation of the information base of the

graphic packets for CAD system and the development of the mathematical model of multivariate system of clothes form obtaining. The analysis of archaeological discoveries has been done, the formal typology and classification has been developed, the structural analysis of Tripill plastics as to the geometrical forms of woman depiction has been given (Figure 3).


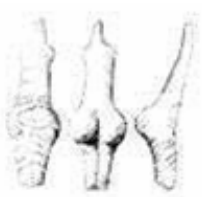

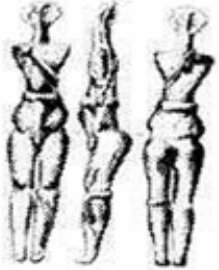
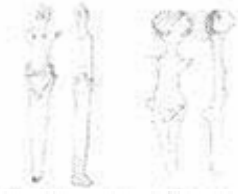
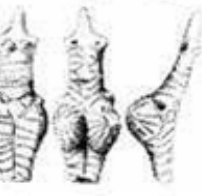
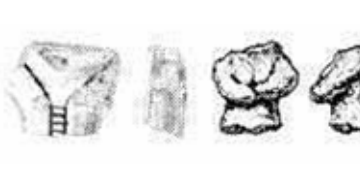
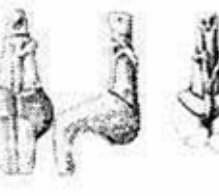
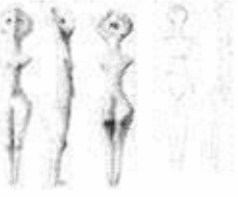

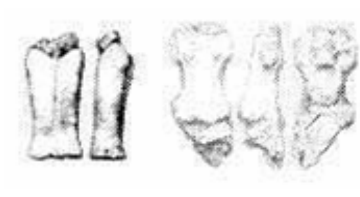
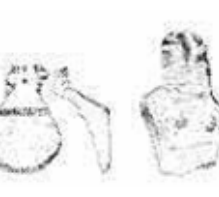
Anthropomorphic statuettes			Variety of modelling
Standing position	Standing position with tilt	Sitting position	
			
			
			

Figure 3 Structural analysis of Tripill plastics as to the geometrical forms of woman depiction

Tripill plastics performed in schematic-natural style are full of symbolism. It is known that the mankind formation was greatly influenced by imaginary world, symbolic realities. Each period of time and each nation have their own values, objects to be symbolized, and their own symbols. The use of signs and symbols is the revealing of national consciousness and the powerful means for its formation as well. The costume is of brightly expressed sign character, determines the ethnic identity in this case. Plastic forms with identified features of clothes silhouette give possibility of clothes form modelling, existed at that time that is why we have developed the morphological matrix of constructive

decorative elements of Tripill clothes. Taking into account the mentioned above statements we have analysed the designing methods and developed product patterns, the relief lines of which are made on the basis of Tripill culture signs, performed modelling and construction of woman clothed (see scheme Figure 4) and developed women clothes collection with the symbols of Tripill culture. The lines of signs are repeated in ready-made articles emphasizing their character, symbolizing protection, wealth and health, and play a very important role in the formation of the modern Ukrainian costume, national consciousness and ethnic self identification.

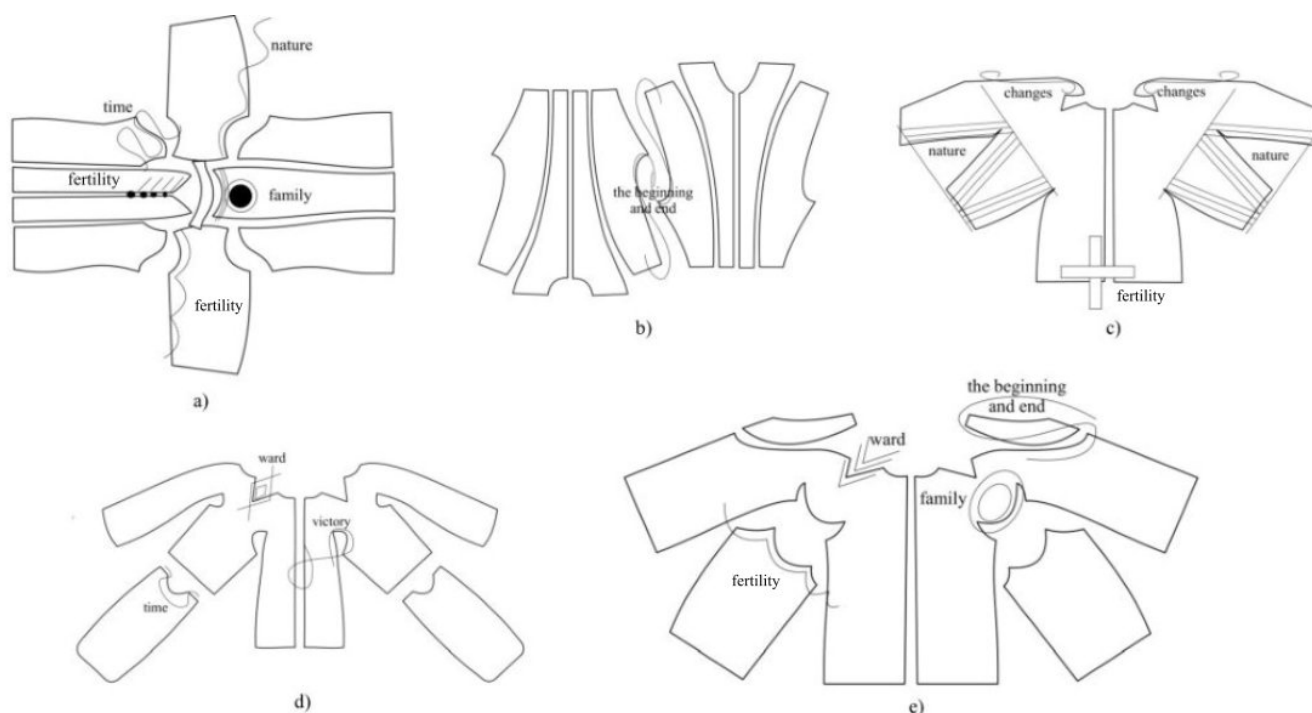


Figure 4 Pattern layout of the women shoulder ferment on the basis of Tripill culture signs: a) nature, time, fertility, family; b) the beginning and end; c) changes, nature, fertility; d) ward, victory, time; e) the beginning and end, ward, family, fertility

4 CONCLUSIONS

Approaches as to the creation of fashion forms of woman clothes using the modern principles and methods of design-modelling with the system of signs and symbols of Tripill culture have been proposed. Combinatorial method of creation of new constructive solutions of the basic elements and their modifications was put into the centre of construction of multivariant compositional set. While using such elements as the silhouette form of the articles, cut and shape of the sleeve, fore-front division, neck-line shape, hem trimming we can obtain 225 variants of the shoulder clothes. These approaches can be applied while creating new forms of clothes including special clothes.

5 REFERENCES

1. Маркевич В.И.: Антропоморфизм в художественной керамике культуры Триполье—Кукутень // Пам'ятники древнейшего искусства на территории Молдавии. — Кишинев, 1989
 2. Погожева А.П.: Антропоморфная пластика Триполья.- Новосибирск, 1983
 3. Петушкова Г.И.: Проектирование костюма: Учебник для высш. учеб. заведений - М.: Издательский центр «Академия», 2004
 4. Колосніченко М.В.: Мода и одяг. Основи проектування та виготовлення одягу. – К.: КНУТД, 2010
1. Markevich V. I. Antropomorfizm v hudozhestvennoj keramike kul'tury Tripol'e—Kukuten // Pamjatniki drevnejshego iskusstva na territorii Moldavii. — Kishinev, 1989
 2. Pogosheva A. P. Antropomorfnaia plastika Tripol'ja.- Novosibirsk, 1983
 3. Petushkova G.I. Proektirovanie kostjuma: Uchebnik dlja vyssh. ucheb. zavedenij. - M.: Izdatel'skij centr «Akademija», 2004
 4. Kolosnichenko M.V. Moda i odjag. Osнови proektuvannja ta vigotvlennja odjagu. – K.: KNU TD, 2010

INSTRUCTIONS FOR AUTHORS

The journal „**Vlákna a textil**“ (Fibres and Textiles) is the scientific and professional journal with a view to technology of fibres and textiles, with emphasis to chemical and natural fibres, processes of fibre spinning, finishing and dyeing, to fibrous and textile engineering and oriented polymer films. The original contributions and works of background researches, new physical-analytical methods and papers concerning the development of fibres, textiles and the marketing of these materials as well as review papers are published in the journal.

Manuscript

The text should be in ***single-column format***.

The original research papers are required to be written in English language with summary. Main results and conclusion of contribution from Slovak and Czech Republic should be in Slovak or Czech language as well.

The other parts of the journal will be published in Slovak language; the advertisements will be published in a language according to the mutual agreement.

The first page of the manuscript has to contain:

The title of the article (16 pt bold, capital letters, centred)

The initials of the **first name** (s) and also **surnames** of all authors (12 pt, normal, centred)

The complete address of the working place of the authors, e-mail of first author (12 pt, italic, centred)

Abstract (10 pt, italic)

Key words (10 pt, italic)

The manuscript has to be written in A4 standard form, in **Arial**.

Do not number the pages and do not use footnotes. Do not use business letterhead.

Figures, tables, schemes and photos should be numbered by Arabic numerals and titled over the table and under the figure or

picture. The total number of figures and tables should not be more than 10.

Photos and schemes have to be sufficiently contrastive and insert in text as pictures.

Mathematical formulae should be centred on line and numbered consecutively on the right margin.

Physical and technical properties have to be quantified in SI units, names and abbreviations of the chemical materials have to be stated according to the IUPAC standards.

References in the text have to be in square brackets and literature cited at the end of the text. References have to contain names of all authors.

1. Surname N., Surname N.: Name of paper or Chapter, In *Name of Book (in Italics)*, Publisher, Place of Publication, YYYY, pp. xxx-yyy
2. Surname N., Surname N.: Name of paper, *Name of Journal (in Italics)* Vol. (No.), YYYY, pp. xxx-yyy
3. Surname N., Surname, N.: Title of conference paper, *Proceedings of xxx xxx*, conference location, Month and Year, Publisher, City, Surname N. (Ed.), YYYY, pp. xxx-yyy
4. Surname N., Surname N.: Name of Paper, Available from <http://www.exact-address-of-site>, Accessed: YYYY-MM-DD

Authors are kindly requested to deliver the paper to be published by e-mail (in Word form).

Address of the Editor Office:

Marcela Hricová

FCHPT, STU in Bratislava

Radlinskeho 9

812 37 Bratislava,

Slovakia

e-mail:

marcela.hricova@stuba.sk